Calhoun: The NPS Institutional Archive

DSpace Repository

Theses and Dissertations 1. Thesis and Dissertation Collection, all items

1997

A comparative study of nuclear technology and direct energy conversion methods for space power systems

Reason, Joseph P., Jr.

Monterey, California. Naval Postgraduate School

http://hdl.handle.net/10945/8110

This publication is a work of the U.S. Government as defined in Title 17, United States Code, Section 101. Copyright protection is not available for this work in the United States.

Downloaded from NPS Archive: Calhoun

DUDLEY KNOX LIBRARY

http://www.nps.edu/library

Calhoun is the Naval Postgraduate School's public access digital repository for research materials and institutional publications created by the NPS community. Calhoun is named for Professor of Mathematics Guy K. Calhoun, NPS's first appointed -- and published -- scholarly author.

Dudley Knox Library / Naval Postgraduate School
411 Dyer Road / 1 University Circle
Monterey, California USA 93943

NPS ARCHIVE
1997
REASON, J.

NAVAL POSTGRADUATE SCHOOL
MONTEREY, CALIFORNIA

THESIS

A COMPARATIVE STUDY OF NUCLEAR TECHNOLOGY AND DIRECT ENERGY CONVERSION METHODS FOR SPACE POWER SYSTEMS

by

Joseph P. Reason, Jr.

June, 1997

Thesis Co-Advisors: Sherif Michael
Barry Leonard

Thesis
R25456

Approved for public release; distribution is unlimited.

DUDLEY KNOX LIBRARY
NAVAL POSTGRADUATE SCHOOL
MONTEREY CA 93943-5101

REPORT DOCUMENTATION PAGE

Form Approved OMB No. 0704-0188

Public reporting burden for this collection of information is estimated to average 1 hour per response, including the time for reviewing instruction, searching existing data sources, gathering and maintaining the data needed, and completing and reviewing the collection of information. Send comments regarding this burden estimate or any other aspect of this collection of information, including suggestions for reducing this burden, to Washington Headquarters Services, Directorate for Information Operations and Reports, 1215 Jefferson Davis Highway, Suite 1204, Arlington, VA 22202-4302, and to the Office of Management and Budget, Paperwork Reduction Project (0704-0188) Washington DC 20503.

1. AGENCY USE ONLY *(Leave blank)*	2. REPORT DATE June 1997	3. REPORT TYPE AND DATES COVERED Master's Thesis

4. TITLE AND SUBTITLE A COMPARATIVE STUDY OF NUCLEAR TECHNOLOGY AND DIRECT ENERGY CONVERSION METHODS FOR SPACE POWER SYSTEMS

5. FUNDING NUMBERS

6. AUTHOR(S) Reason, Joseph, P., Jr.

7. PERFORMING ORGANIZATION NAME(S) AND ADDRESS(ES)
Naval Postgraduate School
Monterey CA 93943-5000

8. PERFORMING ORGANIZATION REPORT NUMBER

9. SPONSORING/MONITORING AGENCY NAME(S) AND ADDRESS(ES)

10. SPONSORING/MONITORING AGENCY REPORT NUMBER

11. SUPPLEMENTARY NOTES The views expressed in this thesis are those of the author and do not reflect the official policy or position of the Department of Defense or the U.S. Government.

12a. DISTRIBUTION/AVAILABILITY STATEMENT
Approved for public release; distribution is unlimited.

12b. DISTRIBUTION CODE

13. ABSTRACT *(maximum 200 words)* The objectives of this thesis are to investigate the theory of direct energy conversion, research the development of space nuclear power systems, evaluate the status of current systems, and draw conclusions about the feasibility and merit of using nuclear power for future space missions. Development of the earliest systems began in 1955 with the Systems for Nuclear Auxiliary Power (SNAP) Program and Project Rover. A detailed review of system design and performance is provided for the reactors and radioisotope thermoelectric generators (RTG's) of past and current programs. Thermoelectric and thermionic energy conversion techniques have been used predominantly in space nuclear power systems. The theory of these direct energy conversion methods is analyzed. Also, the safety review procedures and regulations governing the launch of nuclear sources into space are characterized. Conclusions compare accomplished levels of system performance to theoretically predicted limits and comment on the usefulness of space nuclear power for space applications.

14. SUBJECT TERMS Aerospace Propulsion and Power, Space Vehicles, and Nuclear Energy

15. NUMBER OF PAGES 105

16. PRICE CODE

17. SECURITY CLASSIFICATION OF REPORT Unclassified	18. SECURITY CLASSIFICATION OF THIS PAGE Unclassified	19. SECURITY CLASSIFICATION OF ABSTRACT Unclassified	20. LIMITATION OF ABSTRACT UL

NSN 7540-01-280-5500

Standard Form 298 (Rev. 2-89)
Prescribed by ANSI Std. 239-18 298-102

Approved for public release; distribution is unlimited.

A COMPARATIVE STUDY OF NUCLEAR TECHNOLOGY AND DIRECT ENERGY CONVERSION METHODS FOR SPACE POWER SYSTEMS

Joseph P. Reason, Jr.
Lieutenant, United States Navy
B.S.A.E, U.S. Naval Academy, 1990

Submitted in partial fulfillment
of the requirements for the degree of

MASTER OF SCIENCE IN ASTRONAUTICAL ENGINEERING

from the

NAVAL POSTGRADUATE SCHOOL
June 1997

DUDLEY KNOX LIBRARY
NAVAL POSTGRADUATE SCHOOL
MONTEREY CA 93943-5101

ABSTRACT

The objectives of this thesis are to investigate the theory of direct energy conversion, research the development of space nuclear power systems, evaluate the status of current systems, and draw conclusions about the feasibility and merit of using nuclear power for future space missions. Development of the earliest systems began in 1955 with the Systems for Nuclear Auxiliary Power (SNAP) Program and Project Rover. A detailed review of system design and performance is provided for the reactors and radioisotope thermoelectric generators (RTG's) of past and current programs. Thermoelectric and thermionic energy conversion techniques have been used predominantly in space nuclear power systems. The theory of these direct energy conversion methods is analyzed. Also, the safety review procedures and regulations governing the launch of nuclear sources into space are characterized. Conclusions compare accomplished levels of system performance to theoretically predicted limits and comment on the usefulness of space nuclear power for space applications.

TABLE OF CONTENTS

I. INTRODUCTION 1

II. DIRECT ENERGY CONVERSION 5

- A. THERMOELECTRIC CONVERSION 6
    - 1. Thermoelectric Generator Theory 6
    - 2. Thermoelectric Converter Design 13
- B. THERMIONIC CONVERSION 16
    - 1. Thermionic Generator Theory 16
    - 2. Thermionic Converter Design 21

III. RADIOISOTOPE THERMOELECTRIC GENERATORS (RTG) 25

- A. BACKGROUND 25
- B. RTG DESIGN 27
    - 1. Isotopic Fuel 27
    - 2. Energy Conversion 28
- C. SNAP-3 29
- D. SNAP-9A 30
- E. SNAP-19 31
- F. SNAP-27 34
- G. TRANSIT-RTG 35

H. MULTI-HUNDRED WATT (MHW) GENERATOR 39

I. GENERAL PURPOSE HEAT SOURCE (GPHS) 41

IV. SPACE NUCLEAR REACTORS 43

A. BACKGROUND 43

B. NUCLEAR ROCKET PROGRAM REACTORS 44

C. SNAP NUCLEAR REACTORS 45

1. SNAP-2 45

2. SNAP-10A 50

3. SNAP-8 51

D. OTHER REACTOR DESIGNS 55

1. Fast Reactors 55

2. Advanced Space Nuclear Power Program 56

3. Thermionic Reactors 57

V. CURRENT NUCLEAR REACTOR PROGRAMS 59

A. SP-100 REACTOR PROGRAM 59

B. TOPAZ-II REACTOR SYSTEM 62

C. SUPPORT OF CURRENT PROGRAMS 65

VI. SPACE NUCLEAR SAFETY 69

A. DEVELOPMENT OF EARLY SAFETY PHILOSOPHY 69

1. Technical Staff 69
2. Safety Standards 70
3. Safety Research 70
4. Public Education 70

B. CURRENT SAFETY POLICY 70

1. Radioisotopic Fuel Containment 71
2. Reactor Design and Operation 71
3. Safety Policy of the Former Soviet Union 72

C. SUMMARY OF MISHAPS 74

1. Transit-5BN-3 74
2. Nimbus B-1 74
3. Apollo-13 75
4. Cosmos 954 75

D. INTERAGENCY SAFETY REVIEW 76

1. Accident and Environment Definition 77
2. Source Term 78
3. Environmental Dispersion 79
4. Exposure Pathways 79
5. Radiological Consequences 79
6. Risk Projection 79

VII. CONCLUSIONS 83

A. SAFETY AND REGULATION 83
B. UTILITY OF SPACE NUCLEAR POWER 84
C. RECOMMENDATIONS 85

LIST OF REFERENCES 87

INITIAL DISTRIBUTION LIST 89

LIST OF FIGURES

Figure 1-1. Increasing Power Requirements. From (Angelo and Buden, 1985). 3

Figure 2-1. Thermocouple Circuit. From (Angrist, 1965). 6

Figure 2-2. Simplified Thermocouple. From (Angrist, 1965). 8

Figure 2-3. Junction of Dissimilar Materials. From (Angrist, 1965). 10

Figure 2-4. A Simple Thermoelectric Generator. From (Culp, 1979). 11

Figure 2-5. Thermal Efficiency versus FOM. From (Angelo and Buden, 1985). 13

Figure 2-6. Conductivity of Semiconductors. From (Angelo and Buden, 1985). 15

Figure 2-7. Semiconductor FOM. From (Culp, 1979). 17

Figure 2-8. A Simple Thermionic Generator. From (Culp, 1979). 18

Figure 2-9. A Cesium Vapor Thermionic Converter. From (Angrist, 1965). 22

Figure 2-10. The Effect of the Space-Charge-Barrier. From (Culp, 1979). 23

Figure 3-1. The SNAP-3B RTG. From (Angelo and Buden, 1985). 26

Figure 3-2. The SNAP-9A RTG. From (Angelo and Buden, 1985). 31

Figure 3-3. The SNAP-19 RTG. From (Angelo and Buden, 1985). 32

Figure 3-4. SNAP-27 Fuel Capsule. From (Angelo and Buden, 1985). 34

Figure 3-5. SNAP-27 RTG. From (Angelo and Buden, 1985). 35

Figure 3-6. Transit Thermoelectric Converter. From (Angelo and Buden, 1985). 37

Figure 3-7. MHW RTG Heat Source. From (Angelo and Buden, 1985). 40

Figure 3-8. GPHS RTG. From (Angelo and Buden, 1985). 42

Figure 4-1. The Kiwi-A Reactor. From (Pedersen, 1964). 44

Figure 4-2. SNAP-2 Rankine Cycle Diagram. From (Angelo and Buden, 1985). 46

Figure 4-3. SNAP-2 Reactor Core. From (Angelo and Buden, 1985). 49

Figure 4-4. The SNAP-10A Reactor. From (Corliss, 1966). 51

Figure 4-5. Fluid Loops of the SNAP-8. From (Angelo and Buden, 1985). 53

Figure 4-6. SPR-5 Reactor Heatpipes. 56

Figure 5-1. The SP-100 Reactor. From (Armijo, 1988). 60

Figure 5-2. The SP-100 Reactor Core. From (Murata, 1988). 61

Figure 5-3. The TOPAZ-II Reactor. From (Venable, 1995). 63

Figure 5-4. The TOPAZ-II Reactor Core. From (Venable, 1995). 64

Figure 5-5. Single and Multi-cell Thermionics. From (Benke, 1994). 65

Figure 5-6. Comparison of SP-100 and TOPAZ-II. From (Aftergood, 1988). 67

Figure 6-1. SNAP-10A Fission Products. From (Angelo and Buden, 1985). 73

Figure 6-2. Organization of INSRP. From (Frank et al., 1996). 78

Figure 6-3. The Safety Review Process. From (Frank et al., 1996). 80

Figure 6-4. Risk Assessment Results. From (Frank et al., 1996). 81

Figure 7-1. Methods of Space Power Generation. From (Corliss, 1966). 85

LIST OF TABLES

Table 2-1. Seebeck Coefficients @ 100°C. From (Culp, 1979). 8

Table 2-2. Emission Properties of Materials. From (Culp, 1979). 20

Table 3-1. SNAP RTG Parameters. From (Angelo and Buden, 1985) 38

Table 4-1. Summary of SNAP Reactors. From (Corliss, 1966). 54

Table 7-1. Current Use of Space Nuclear Power. From (Gray, 1993). 85

I. INTRODUCTION

Since the beginning of this country's space program, designers of spacecraft have experienced a steadily growing need for greater amounts of electrical power. Compared to other components of a spacecraft, the power system is usually quite heavy. Methods of increasing the power density of such systems have always been of great interest. There are types of space missions that push the limits of power generating technology in terms of power required and the duration of the mission. These can be earth-orbiting satellites or they can be deep-space exploration spacecraft. In both cases, and in others, the life of the power system, determines the life of the spacecraft. The technologies of solar cells, fuel cells, and batteries are constantly advancing and the scope of application of these methods is broadening. However, space missions that involve the exploration of deep space using autonomous probes or manned vehicles require levels of power generation and system lifetimes that cannot be attained by these conventional techniques. Figure 1-1 illustrates increasing power requirements of space missions.

Chapter II conducts a theoretical analysis of the two energy conversion methods employed by the space nuclear power systems, thermoelectrics and thermionics. The potential for advances in the thermal efficiency and power output of these technologies determines the benefits of using them in the near future. Understanding the technical history and operating principles of space nuclear power is important to evaluating the feasibility and effectiveness of reactors and thermoelectric generators.

In 1955, the Atomic Energy Commission began to investigate the use of nuclear power sources to further our purposes in space exploration with the Systems for Nuclear Auxiliary Power (SNAP) Program and the program to design a nuclear rocket (Project Rover). The space nuclear power systems that were developed were either radioisotope thermoelectric generators (RTG's) or space nuclear reactors. Chapter III explores the development and operation of RTG's. Chapter IV does the same for space nuclear reactors. More attention is paid to programs which made significant contributions to present technology. Chapter V addresses status of current space reactor programs to demonstrate present power generating capabilities.

Considering the use of nuclear power in space raises many questions. Cost is of concern because the systems are very expensive to develop and build. Significant benefits are needed to justify the cost and difficulty of designing nuclear power systems. The question of safety is prominent, especially for manned space missions.

An understanding of the safety philosophy, safety review process, and legislation that govern the design and use of space nuclear systems is equally important. Chapter VI explains the original safety policy of our space program and the Presidential directives that have modified it. The chapter also describes the current safety review process and summarizes mishaps that have occurred involving nuclear powered spacecraft.

The purpose of this thesis is to research the technical development of space nuclear power systems, analyze the theory of their operating principles, and evaluate the effectiveness of safety measures and review efforts. The conclusions, drawn in Chapter VII, focus upon the usefulness of nuclear power for space exploration.

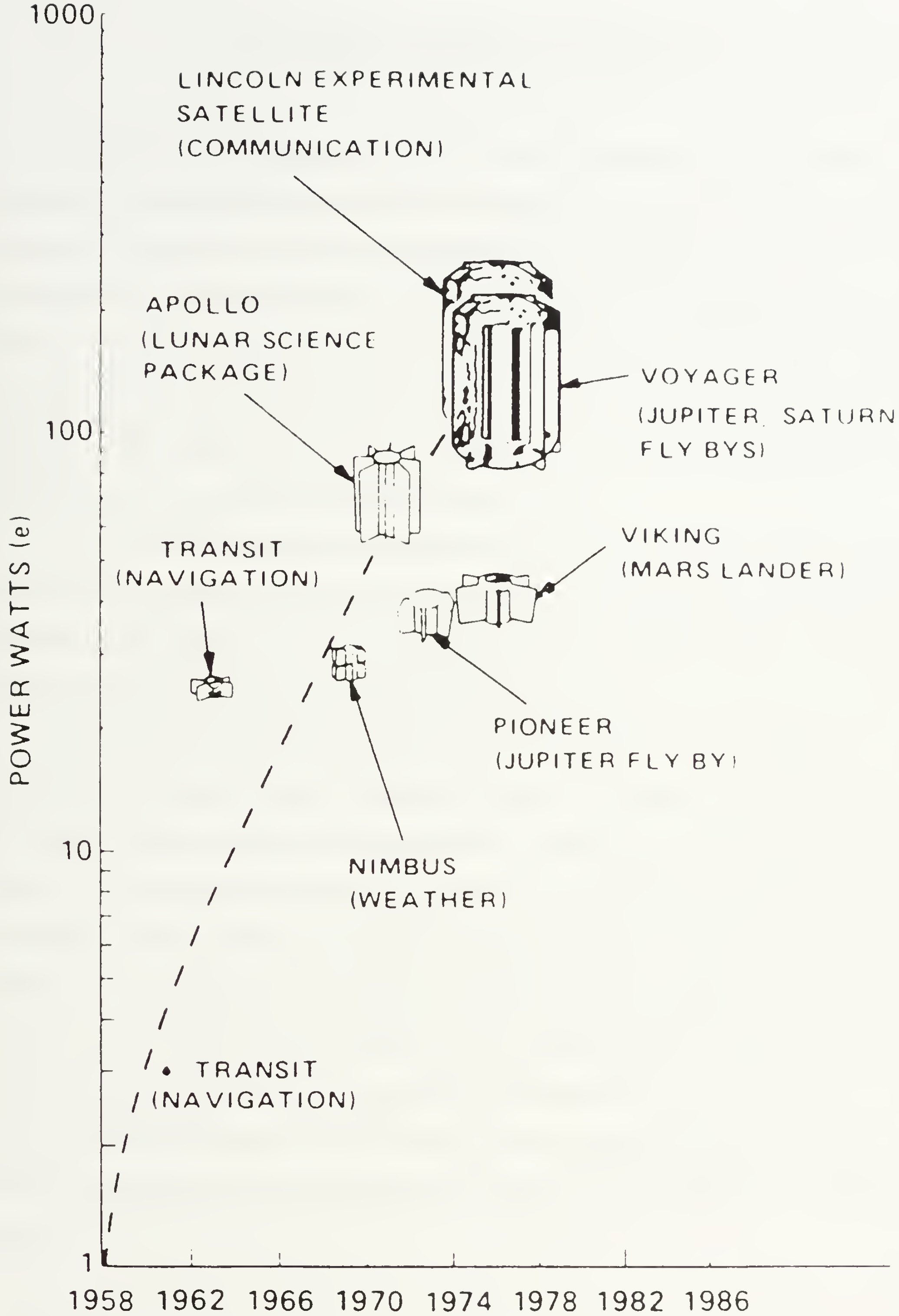

Figure 1-1. Increasing Power Requirements. From (Angelo and Buden, 1985).

II. DIRECT ENERGY CONVERSION

Photovoltaic generators are by far the most common power systems in space applications. Fuel cells have also been used extensively since the years of the Apollo lunar missions. Magnetohydrodynamic generators (MHD) can also be considered. An MHD operates by using the kinetic energy of a plasma stream moving through a magnetic field to induce an electrical field in the stationary conductor of a generator (Angrist, 1965). The simplicity of this concept make MHD's attractive to space power system design. However, significant technological advances will be required to overcome the difficulties in designing an MHD that can be applied practically (Venable, 1995).

In the search for methods of generating significantly larger amounts of power for space missions, nuclear energy has great potential. To harness this potential, the thermal energy released during the decay of radioactive isotopes and controlled nuclear reactions must be converted into electricity with maximum efficiency.

The conversion of thermal energy into electricity can be accomplished by a number of methods. In a Rankine cycle converter, a heat source transfers heat to a working fluid. The working fluid is expanded through a turbine, which turns an alternator and generates electricity. The goal of direct energy conversion is to eliminate the intermediate (turbines, etc.) steps in order to increase converter efficiency. Space nuclear power systems can be divided into two categories, radioisotope thermoelectric generators (RTG's) and space nuclear reactors. An RTG uses the direct method of thermoelectric energy conversion, space reactors may use either a direct energy conversion method or one of the indirect methods such as, a Brayton or Rankine cycle. Thermoelectric and thermionic generation are currently the direct energy conversion methods most important to the support of advanced space missions.

A. THERMOELECTRIC CONVERSION

1. Thermoelectric Generator Theory

A thermoelectric generator functions on the principles of several important discoveries. They are the Seebeck effect, the Peltier effect, and the Thomson effect. They will each be described in detail as it becomes necessary in explaining the operation of a thermoelectric converter. In 1822, German physicist, Thomas J. Seebeck observed that when two dissimilar materials are joined to form a circuit and a temperature gradient is maintained across the two junctions, a voltage is produced. The Seebeck coefficient of each material describes the rate at which thermoelectric potential across the material changes with temperature. (Culp, 1979)

Consider the thermocouple circuit illustrated in Figure 2-1. Two dissimilar materials, A and B, are joined together at one end, point 5 in the circuit. At this junction, both materials are exposed to a heat source with temperature, T_H. The other ends of the materials, points 3 and 4, rest in an ice bath that maintains them at a colder temperature T_C.

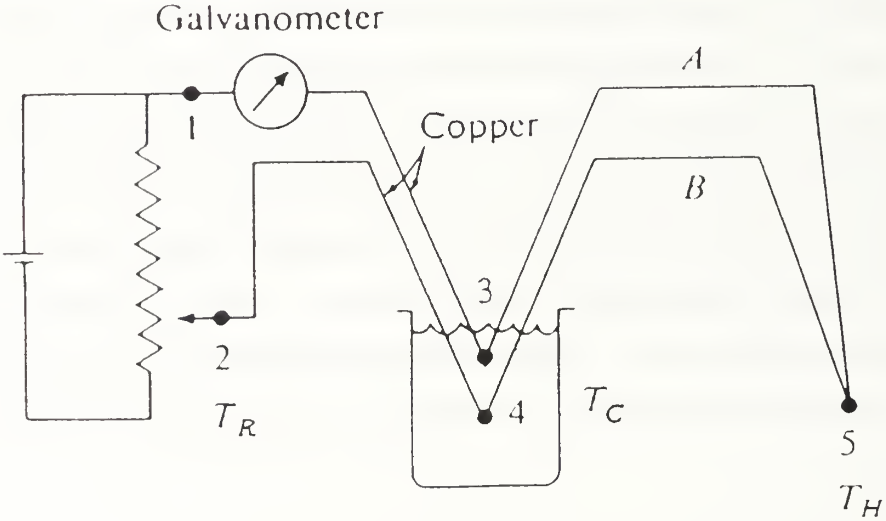

Figure 2-1. Thermocouple Circuit. From (Angrist, 1965).

Copper wires lead from the cold ends of the materials to the terminals of a potentiometer at points 1 and 2. When the potentiometer is balanced (zero current through the galvanometer) a potential difference is noted between material A and material B at points 3 and 4. This is the Seebeck voltage and it is caused by the temperature gradient, T_H-T_C, and the differing Seebeck coefficients of the materials. For each material, the Seebeck coefficient is given by the following expression where, E_S is the potential (in volts) and T is the temperature in (K). (Angrist, 1965)

$$S = dE_S / dT \qquad (2\text{-}1)$$

The electric potentials of materials A and B at the cold ends are different because their thermoelectric potentials change at different rates as temperature changes.

To illustrate how this happens, Figure 2-2 shows a simplified drawing of the same thermocouple. The five numbered points correspond to the points in Figure 2-1. Both materials A and B are subjected to the same temperature gradient. There are steady-state temperature differences along the length of material A. When added together, they equal the temperature difference between points 3 and 5. The Seebeck effect causes a corresponding potential difference between points 3 and 5. The same is true for material B. At point 5, materials A and B share the same electric potential and temperature. At points 3 and 4, they share the same temperature, but their electric potentials will be different because of their differing Seebeck coefficients. (Angrist, 1965)

When the Seebeck coefficients of both materials in a circuit and temperature gradient across the junctions are known, the thermoelectric potential produced is given by the equation,

$$E = \int (S_a - S_b)\, dT \qquad (2\text{-}2)$$

In this equation, $(S_a - S_b)$ is the effective Seebeck coefficient, S_{ab}. Table 2-1 gives the Seebeck coefficients for a selection of materials. (Culp, 1979)

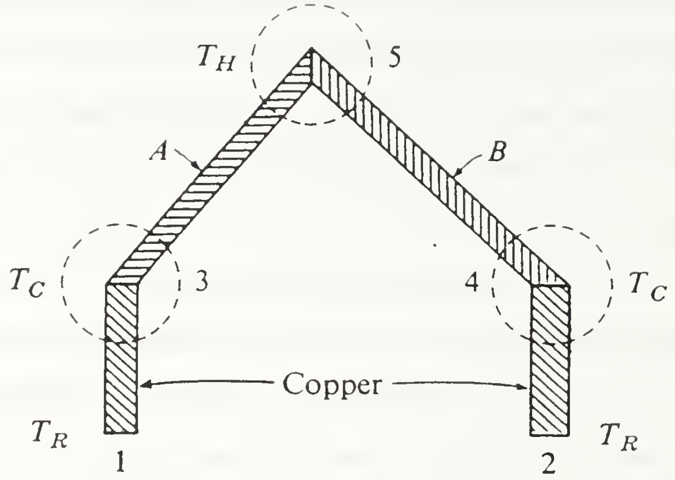

Figure 2-2. Simplified Thermocouple. From (Angrist, 1965).

Material	S, V/K
Aluminum	-0.2×10^{-6}
Constantan	-47.0×10^{-6}
Copper	$+3.5 \times 10^{-6}$
Iron	$+13.6 \times 10^{-6}$
Platinum	-5.2×10^{-6}
Germanium	$+375.0 \times 10^{-6}$
Silicon	-455.0×10^{-6}

Table 2-1. Seebeck Coefficients @ 100°C. From (Culp, 1979).

Considering these values and Equation 2-2, it can be understood that, for a given ΔT, the amount of thermoelectric potential induced is greatest when material A has the most positive Seebeck coefficient and material B has the most negative Seebeck coefficient. Coefficient magnitudes are greatest for semiconducting materials. The Seebeck effect is still observable in other materials, such as metal alloys, but it is inadequate for use as an electrical power source. Lead telluride is an effective material combination as are other n-p semiconductors.

Through a process called doping, impurity atoms are injected into the lattice of a material. When the impurity atoms have one more electron than the number needed to form a valent bond with the material being doped, a n-type semiconductor is formed. When the impurity atoms have one fewer electron than the number needed to form a valent bond, holes are introduced into the material lattice and a p-type semiconductor is formed. Note a that neither semiconductor carries a net charge. The n-type material simply has extra electrons embedded in its lattice and the p-type material has extra "holes" for electrons embedded in its lattice. The extra electrons and the holes move towards the cold junction where they accumulate and combine. If material A is the p-type semiconductor and material B is the n-type semiconductor the effective Seebeck coefficient becomes, $S_{ab} = S_{p}n$ and the expression for the Seebeck voltage can be rewritten. (Culp, 1979)

$$E_s = \int S_{p}n \, dT \qquad (2\text{-}3)$$

Figure 2-3 is a schematic of a single junction of dissimilar materials. In 1844, French physicist, J. C. A. Peltier observed that when direct electric current, I, flows from material A to material B , heat is given off from the junction. This differs from the expected, $I(V_a - V_b) = I^2R_j$, where R_j is the junction resistance. The difference between heat currents, Iq_a and Iq_b, is noted as Iq_j. From an energy balance:

$$Iq_j = I^2R + Iq_a - Iq_b \qquad (2\text{-}4)$$

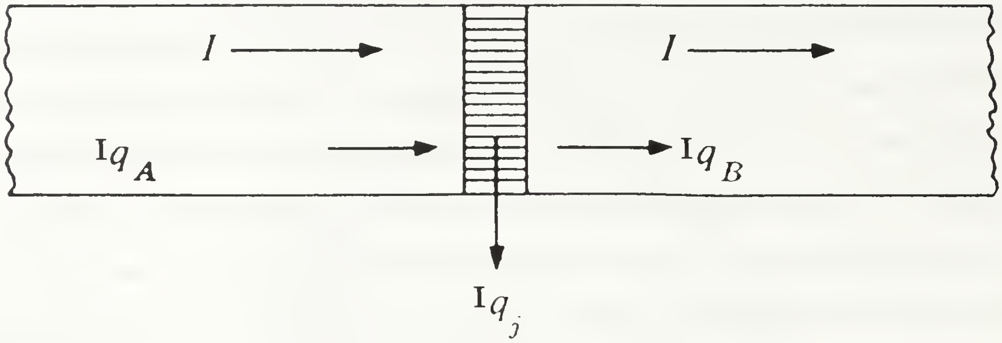

Figure 2-3. Junction of Dissimilar Materials. From (Angrist, 1965).

The Peltier heat, Q, is defined as the difference between Iq_a and Iq_b or,

$$Iq_a - Iq_b = Iq_j - I^2R = \pi_{ab} I \qquad (2\text{-}5)$$

where π_{ab} is called the Peltier coefficient. (Zemansky, 1957)

The following expression defines the Peltier coefficient , π_{ab} ,where -Q is the rate of heat transfer from the junction and I denotes the generator current (Culp, 1979).

$$\pi_{ab} = -Q/I \qquad (2\text{-}6)$$

The following equation relates the Peltier coefficient to the Seebeck coefficient where T_j is the absolute temperature of the junction.

$$\pi_{ab} = T_j S_{ab} = T_j (S_a - S_b) \qquad (2\text{-}7)$$

The sign of π_{ab} is positive when the current flows from material A to material B.

In 1854, English physicist, William Thomson (Lord Kelvin) observed the reversible absorption or liberation of heat that occurred when a homogeneous conductor was subjected to simultaneous electrical and temperature gradients. Although this effect does not directly influence the operation of a thermoelectric converter, it aids in general understanding. This following equation defines the Thomson coefficient and relates it to the Seebeck effect where Q is the heat transfer rate,

$$\tau = (Q / I)\,\Delta T = T\,(dS / dT) \qquad (2\text{-}8)$$

Figure 2-4 is a basic diagram of a thermoelectric generator. The arrows illustrate the direction of heat flow in and out of the semiconductor junctions.

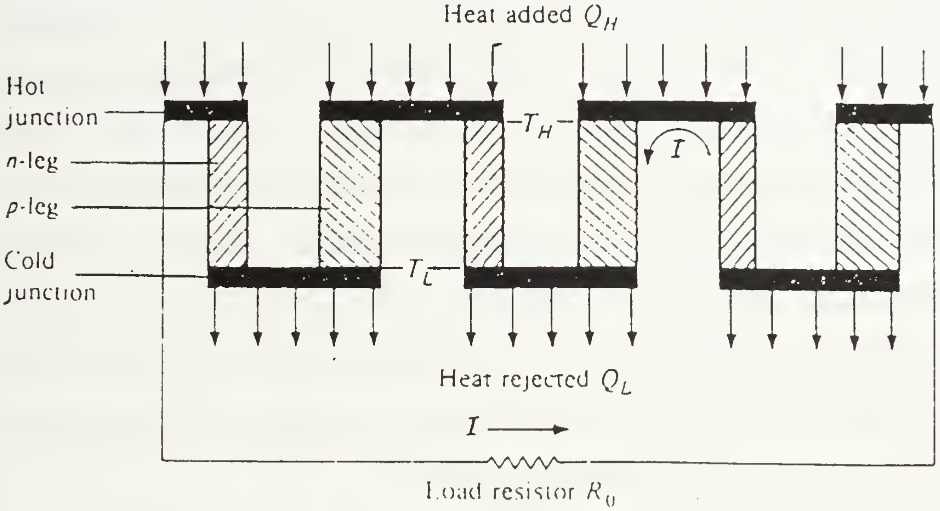

Figure 2-4. A Simple Thermoelectric Generator. From (Culp, 1979).

Current flows from the p-leg to the n-leg at the cold junctions of the generator in Figure 2-4. This defines the combined Seebeck coefficient for the system, S_{pn}, as a positive value. Also note that the elements of the generator are connected in series for electrical current and in parallel for heat flow. The total electrical resistance of the generator, R_g, is calculated by summing the resistances of the elements along the path of current flow and m is the number p-n legs in the generator. The resistances of the metallic connections at the hot and cold junctions are neglected and the equation becomes,

$$R_g = m\,(R_p + R_n) \qquad (2\text{-}9)$$

The resistances of the p-leg and the n-leg are calculated the total area of the leg, A, the length of each leg and the resistivity of the leg material, ρ, using the equation,

$$R_p = (\rho_p L_p)/A_p \qquad R_n = (\rho_n L_n)/A_n \tag{2-10}$$

The total conductance of the generator, K_g, is calculated similarly. Recall that conductance of the material, k, is simply the inverse of its thermal resistivity. Equations 2-7 and 2-8 become,

$$K_g = m(K_p + K_n) \tag{2-11}$$

$$K_p = (k_p A_p)/L_p \qquad K_n = (k_n A_n)/L_n \tag{2-12}$$

There are four terms in an energy balance of each junction in the thermoelectric generator. Consider the case of the hot junction. Heat is being transferred from a source at the rate, Q. This heat travels through the generator to the cold junction. The rate of heat flow (neglecting radiative heat transfer) is dependent upon the thermal conductance of the generator, K_g. The resulting term in the energy balance is $K_g\Delta T$. Current, I, flowing through the generator causes cooling in the hot junction at a rate determined by the product of the current and the Peltier coefficient, π_{ab}. The heat transfer rate due to the Peltier effect, $mS_{pn}T_hI$, is more easily calculated by from the Seebeck coefficients of the generator components where, S_{pn} is given by the following equation,

$$S_{pn} = \int [(S_p - S_n)/\Delta T]dT \tag{2-13}$$

Lastly, power will be dissipated as a result of Joule heating. The total amount of Joule heating is given by, I^2Rg, and occurs equally at both junctions due to the flow of current and the electrical resistance of the generator. Combining these terms results in the energy balance for the hot junction of a thermoelectric generator.

$$Q_H = mS_{pn}T_H I + K_g\Delta T - I^2R_g/2 \tag{2-14}$$

The thermal power transferred to the environment at the cold junction is given by,

$$-Q_L = mS_{pn}T_L I + K_g\Delta T + I^2R_g/2 \tag{2-15}$$

The thermal efficiency of the generator is the ratio of the power dissipated in the load to the power transferred to the hot junction from the heat source. (Culp, 1979)

$$\eta_{th} = I^2R_O/Q \tag{2-16}$$

Performance of a generator depends upon the material properties of its components, its electrical resistance, and its thermal conductance. A quantitative measure of the degree to which these variables are optimized is given by Z, the thermoelectric generator figure of merit (FOM). (Culp, 1979)

$$Z = (m^2 S_{pn}^2) / (K_g R_g) \qquad (2\text{-}17)$$

2. Thermoelectric Converter Design

The FOM of a thermoelectric generator is an important design parameter which relies most heavily upon the component materials selected. As Figure 2-5 demonstrates, even small increases in FOM can result in significant increases of the thermal efficiency and coefficient of performance of the converter. In the figure, T_{av} is the average temperature between T_H and T_C.

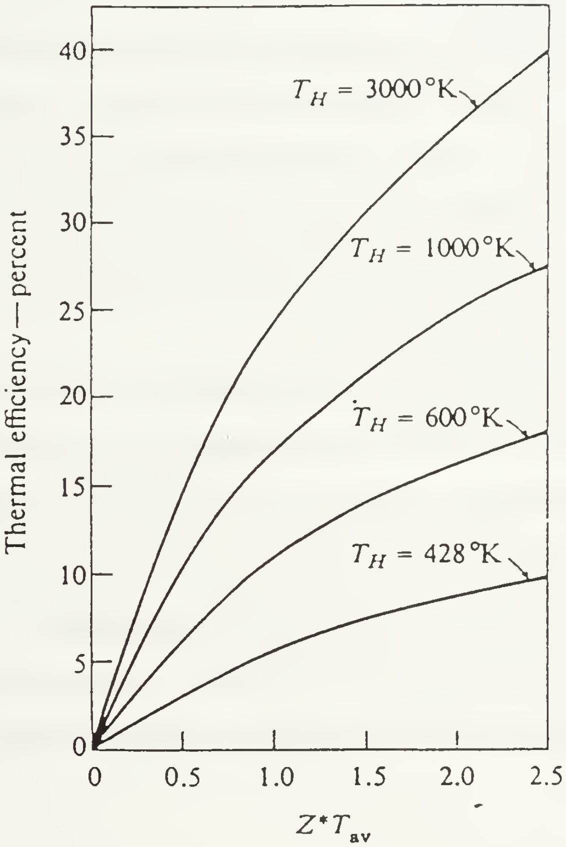

Figure 2-5. Thermal Efficiency versus FOM. From (Angelo and Buden, 1985).

This makes the development of new materials crucial to the advancement of thermoelectric generator technology. For a single material, the FOM is,

$$Z = S^2 / \lambda_p \qquad (2\text{-}18)$$

Where, λ_p is constant for a material. So generally, the larger the Seebeck coefficient, the greater the FOM. (Angrist, 1965)

Certain semiconductors have higher FOM than any metal, however, these materials do not exhibit the same performance levels at all temperatures. In selecting materials, three characteristics must be optimized over the temperature range of interest. They are the material's Seebeck coefficient, electrical resistivity, and thermal conductivity. These quantities are functions of the charge carrier concentration. Figure 2-6 illustrates these relationships. (Angrist, 1965)

Thermoelectric generator technology benefitted greatly from the lessons learned about semiconductors through the development of transistors. New lattice materials, new doping materials, and improvements in doping techniques have led to the development of semiconductors capable of operating at higher temperatures with higher FOM. Still, no one material operated very well over a broad temperature range (Pedersen, 1964). Figure 2-7 shows the FOM of some selected materials.

The use of telluride materials in thermoelectric converters began early in this country's space nuclear power history. Lead telluride and silver-antimony-germanium telluride are proven performers. However, the tellurides do not operate well above temperatures of 800 K. This is limiting as greater power requirements continue to demand higher operating temperatures. At high temperatures, generator components have been observed to sublimate, degrading thermal efficiency. This occurs primarily at the hot junction. Silicon germanium materials have demonstrated the ability to operate at much

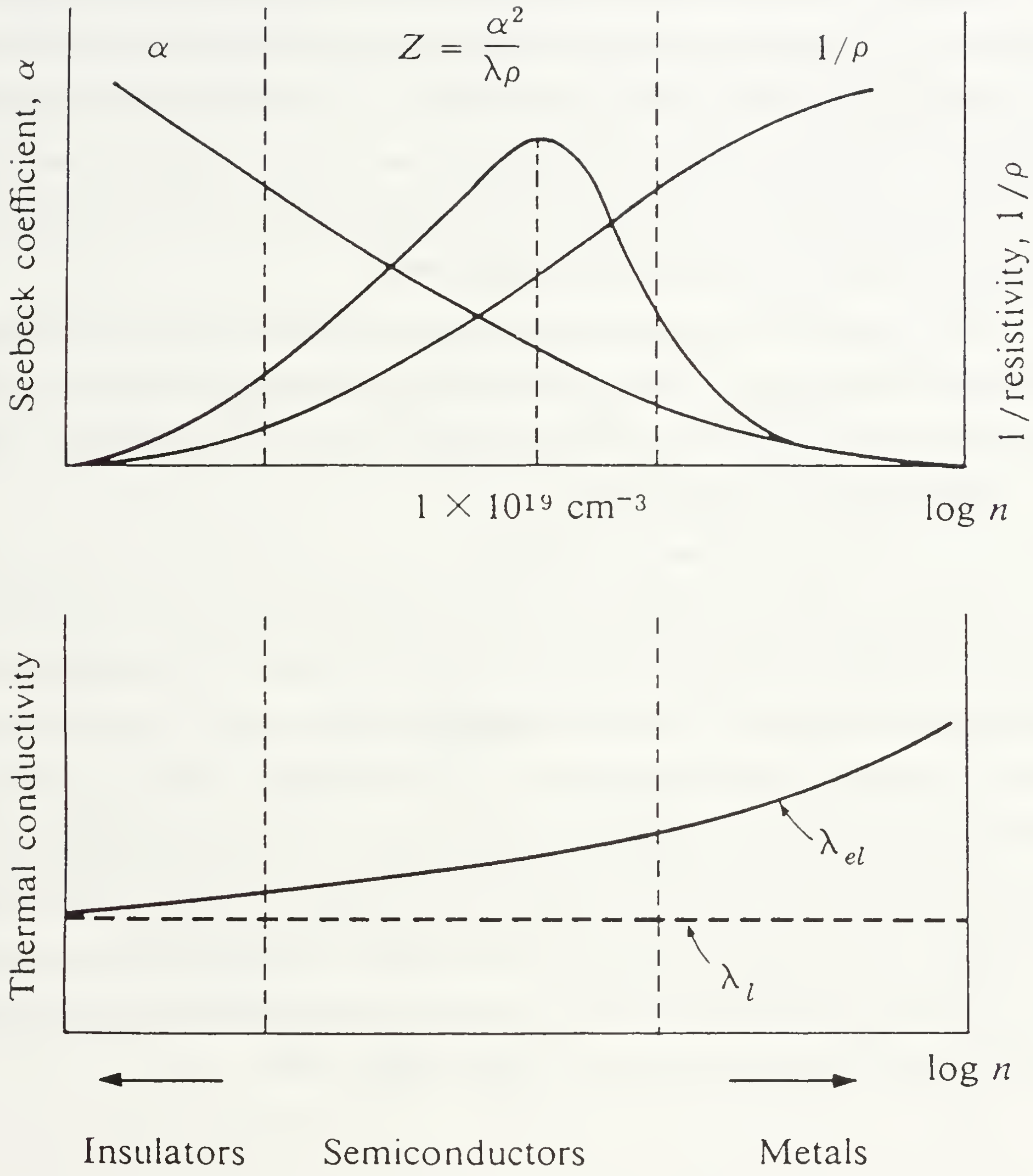

Figure 2-6. Conductivity of Semiconductors. From (Angelo and Buden, 1985).

higher temperatures. Possible methods of enhancing the SiGe figure of merit include doping with materials, such as gallium-phosphorus. (Angelo, 1985)

In addition to thermal and electrical performance parameters, there are several design issues that must be addressed when selecting materials for a thermoelectric generator. Construction of a converter requires semiconductor-to-metal interfaces. These interfaces must provide for the free flow of heat and electricity. The converters operate at very high temperatures. Thermal compression and expansion can introduce significant mechanical stresses. Semiconductors are relatively weak materials, methods such as compressive loading must be used to account for this. (Angrist, 1965)

These problems of mechanical and thermal performance degrade theoretically attainable efficiencies by 20% - 50%. With continued improvements in material technology and innovations such as ion coating, efficiencies of 30% may be reached (Pedersen, 1964).

B. THERMIONIC CONVERSION

1. Thermionic Generator Theory

Thomas A. Edison is credited with discovering thermionic emission in 1883. He observed that when a strip of conducting material was held within the globe of an incandescent electric lamp, close to the incandescent filament, current flowed in the strip. This flow of negative electricity became known as the Edison effect. In 1899, J. J. Thomson observed that an incandescent conductor in a vacuum emitted negatively charged particles that matched the charge to mass ratio of electrons. It was not until 1933, that Langmuir demonstrated sufficient understanding of these principles to build a thermionic converter. This technology did not begin to truly progress until Hastopulous described thermionic converters in detail in his doctoral thesis of 1956 (Angrist, 1965).

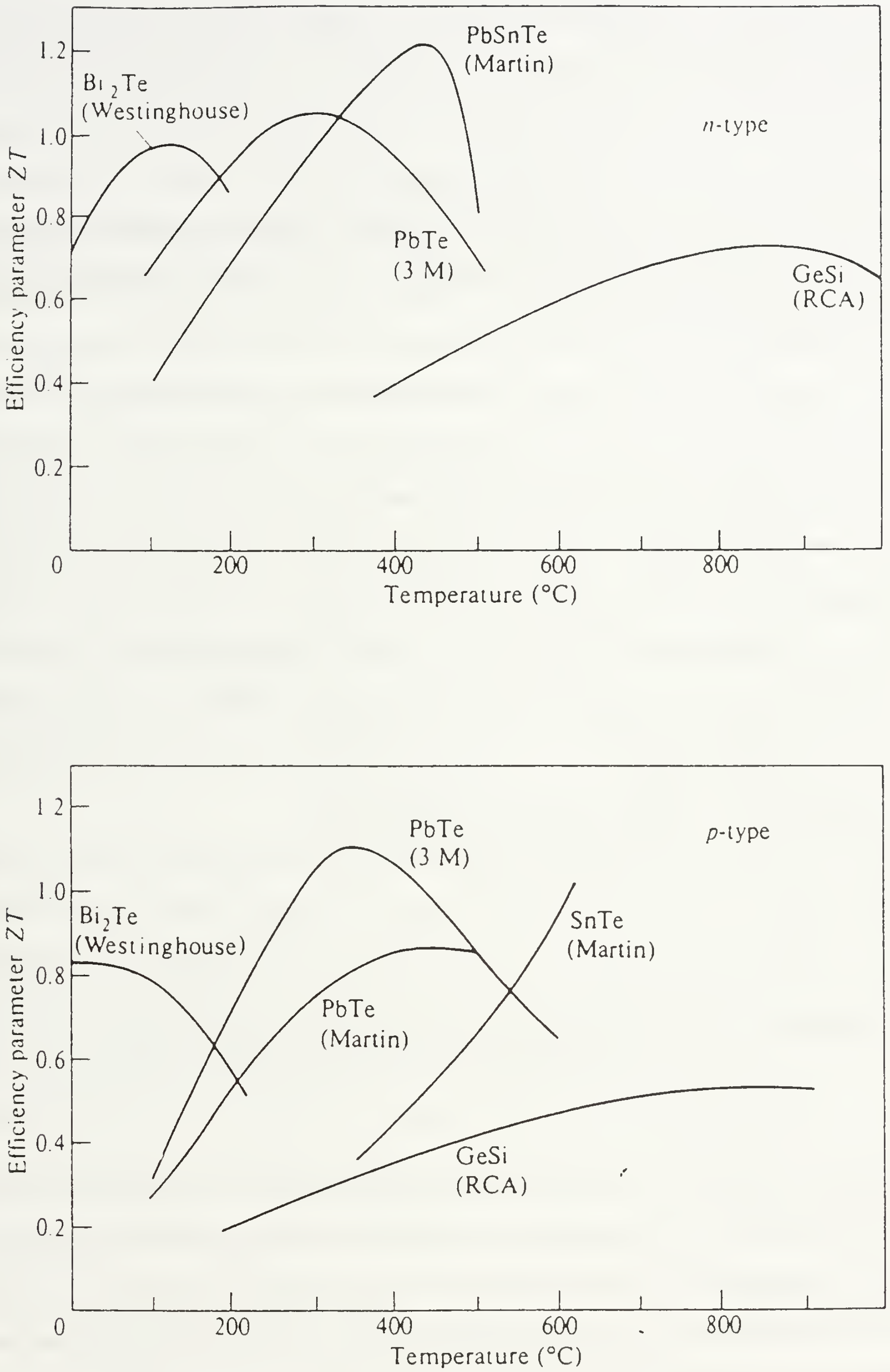

Figure 2-7. Semiconductor FOM. From (Culp, 1979).

The fundamental components of a thermionic generator are a hot anode, called an emitter, and a cold cathode, called a collector. As demonstrated by the Edison effect, when heated to incandescence, the hot anodic material will "boil off" electrons. In a vacuum, these electrons will cross a small gap and condense on the surface of the cathode. This produces a potential difference between the emitter and the collector. If the two are joined electrically, current will flow through a resistive load. Figure 2-8 is a schematic illustrating the basic principles of a thermionic converter.

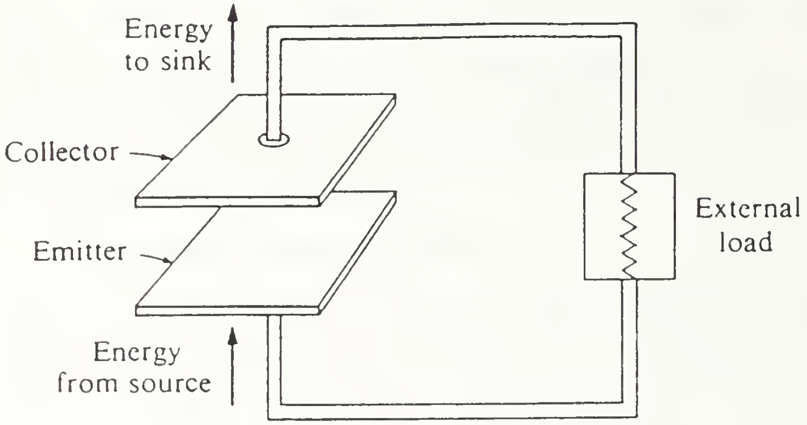

Figure 2-8. A Simple Thermionic Generator. From (Culp, 1979).

The valence electrons of an atom vibrate about the nucleus at a specific energy level, known as the Fermi-level. The amplitude of the Fermi-level energy increases and decreases with absolute temperature. For these electrons to cross the gap to the collector, several obstacles must be overcome. Energy is required to strip an electron away from its nucleus. This is known as the work-function energy, ϕ. The work-function and the Fermi-level energies are properties of a material. With these principles, it is possible to calculate the thermal emission rate of electrons leaving the surface a cathode. This quantity is expressed as a current density, J_0, and is calculated using the Richardson-Dushman equation (Culp, 1979),

$$J_o = \xi T^2 \exp [(-e\phi) / (kT)] \qquad (2\text{-}19)$$

In this equation, k is the Boltzman constant, e is the charge of an electron, T is the absolute temperature, ϕ is the work-function in electron-volts, and the constant ξ is a material property of the emitter. When electrons leave the surface of the emitting cathode, the cathode becomes positively charged. This charge attracts the electrons that are released. As electrons are released, they accumulate in the gap between the cathode and the anode. The electrons that are already in the gap repel those that are just released from the anodic surface, tending to push them back towards the anode. The barrier that forms from the combination of these effects is called the space-charge-barrier. To cross the gap and reach the cathode, an electron must overcome the work-function energy, ϕ_c, and the energy of the space-charge-barrier, ϕ_b. Considering these obstacles, the expression given for current density at the cathode becomes (Culp, 1979),

$$J_o = \xi T^2 \exp [(-e(\phi_c + \phi_b) / (kT)] \qquad (2\text{-}20)$$

Figure 2-8 shows an energy diagram for a simple thermionic-diode generator. Note from the diagram that the output voltage of a converter must be equal to the energy at the anode subtracted from the energy at the cathode. Selection of converter materials is a key factor in maximizing the output of a generator. The cathode should have a low Fermi-level and a high work function. The anode should have a high Fermi level and a low work function. Table 2-2 provides the thermionic emission properties of selected materials.

Material	ϕ, V	ξ, $A/m^2 \cdot K^2$
Cs	1.89	0.50×10^6
Mo	4.2	0.55×10^6
Ni	4.61	0.30×10^6
Pt	5.32	0.32×10^6
Ta	4.19	0.55×10^6
W	4.52	0.60×10^6
W + Cs	1.5	0.03×10^6
W + Ba	1.6	0.015×10^6
W + Th	2.7	0.04×10^6

Table 2-2. Emission Properties of Materials. From (Culp, 1979).

The optimal relationship between temperature and work function is (Culp, 1979),

$$\phi_a / T_a = \phi_c / T_c \qquad (2\text{-}21)$$

There are three primary power losses from the cathode of a thermionic generator. There is radiative heat transfer between the cathode and the anode. This term, P_r, is calculated by assuming that the gap between the electrodes is very small and that the cathode and anode can be considered to be infinite plates. The "boiling off" of electrons causes additional power loss at the cathode, P_{el}. At a given current density, J_0, the power loss due to the flow of electrons is,

$$P_{el} = J_o A_c \left(\phi_c + \phi_{b,c} + (2kT_c) / e\right) \qquad (2\text{-}22)$$

The third source of power loss is associated with the lead wire that connects the cathode to the heat source. If the wire has a thermal conductance, k_W, cross-sectional area, A, electrical resistivity, ρ, and length, L, the power loss due to the combination of conduction heat transfer and Joule heating rate to the cathode is given by the expression:

$$P_W = (kA / L)(T_c - T_o) - [(J_o A_c)^2 (\rho L / A)] / 2 \qquad (2\text{-}23)$$

With these three loss terms and the power output of the generator, the equation for the thermal efficiency of the converter becomes,

$$\eta_{th} = P_{out} / (P_r + P_{el} + P_W) \qquad (2\text{-}24)$$

2. Thermionic Converter Design

The type of thermionic generator described in the previous section is known as an ideal vacuum diode. The vacuum refers to the gap between the cathode and the anode. The ideal vacuum diode represents the upper bound of thermionic converter design because the methods used to measure its performance neglect some effects that degrade converter efficiency. At the high temperatures of operation, the hot cathode tends to deteriorate (Culp, 1979). The temperature of the anode is also of concern. High collector temperatures are desirable for space systems because heat rejection relies completely upon radiation into a vacuum. However, if the collector temperature is too high, electrons will be emitted back into the cloud of electrons flowing from the emitter. This back emission can be compensated for by increasing the work function of the collector or by increasing the number of electrons "boiled off" by the emitter. This is a design trade-off because raising the collector temperature will, generally, lower converter efficiency (Angelo and Buden, 1985). Another design issue is the presence of the space-charge-barrier. Electrons leaving the emitter collide with one another and create a charged region in the gap between the electrodes which impedes the flow to the collector. This gap is very small. Any misshaping of the electrodes due to thermal expansion of components can effectively short this small tolerance. The interelectrode gap introduces complications of a mechanical and electrical nature into the design of a thermionic converter. (Angrist, 1965)

One way to allow converters to be constructed with a larger interelectrode gap and counteract the effect of space charge forces simultaneously is to fill the gap with a plasma. This type of thermionic converter is called a plasma diode. Cesium gas is most often used in this design. The cesium gas, when heated, produces positive ions in the gap between the emitter and the collector. The negative charge of the cloud of electrons is neutralized and the electrons are able to travel a greater distance to the collector. Cesium is a good choice because it has the lowest potential of any element and ions are formed easily. By varying the pressure of the cesium vapor, a range of emitter work functions can be attained at a given temperature (Angelo and Buden, 1985). Figure 2-9 shows a gas filled converter.

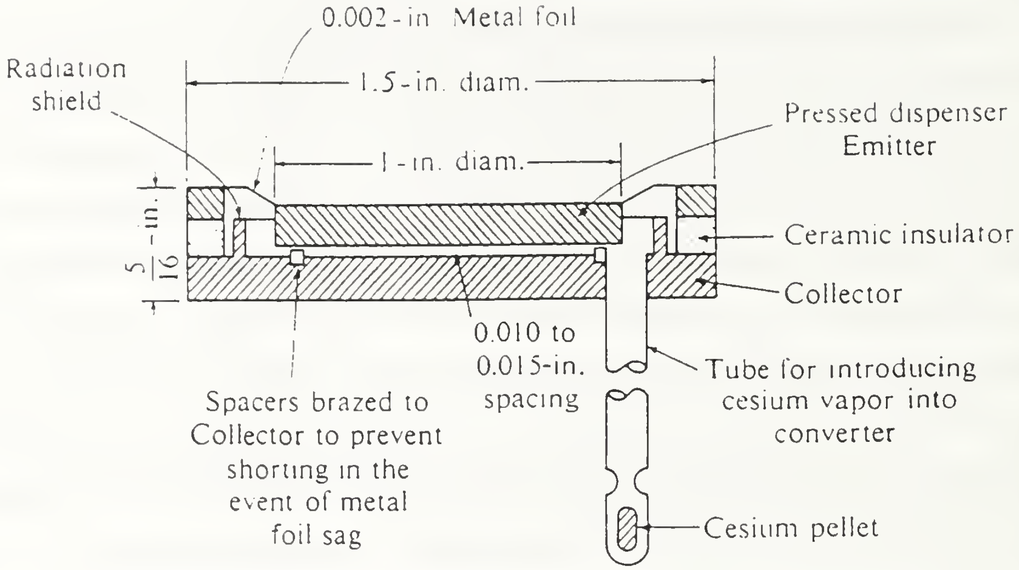
0.002-in Metal foil
Radiation shield
1.5-in. diam.
Pressed dispenser Emitter
1-in. diam.
5/16-in.
Ceramic insulator
Collector
0.010 to 0.015-in. spacing
Tube for introducing cesium vapor into converter
Spacers brazed to Collector to prevent shorting in the event of metal foil sag
Cesium pellet

Figure 2-9. A Cesium Vapor Thermionic Converter. From (Angrist, 1965).

Cesium ions are formed inside the generator in two ways. One of these occurs in each of the three modes of operation of a cesium vapor converter. In the low pressure mode, the vapor pressure is low and the emitter temperature is high enough for cesium ions to form due to contact with the emitter surface. In the high pressure mode, cesium covers the cathode and the anode reducing their workfunctions to more optimal values. These first two modes of operation are called unignited modes. In the third, ignited mode, cesium ions are formed by collisions with electrons. In this mode, the thermionic converter reaches it highest levels of power and efficiency. (Angrist, 1965)

Thermionic converter performance will improve with advances in methods of reducing electrode gaps, lowering collector work functions, and decreasing the voltage drop experience by a generator operating in the ignited mode. Figure 2-10 shows the dependency of thermal efficiency upon reduction of the voltage drop across the space-charge-barrier, V_B (Angrist, 1965).

Typical cesium thermionic converters attain thermal efficiencies of 15% - 20%. This is higher than the levels commonly achieved by thermoelectric methods. However, thermionic systems are less rugged, difficult to build, and very expensive. Future developments should make theoretical efficiencies of up to 30% achievable. (Culp, 1979)

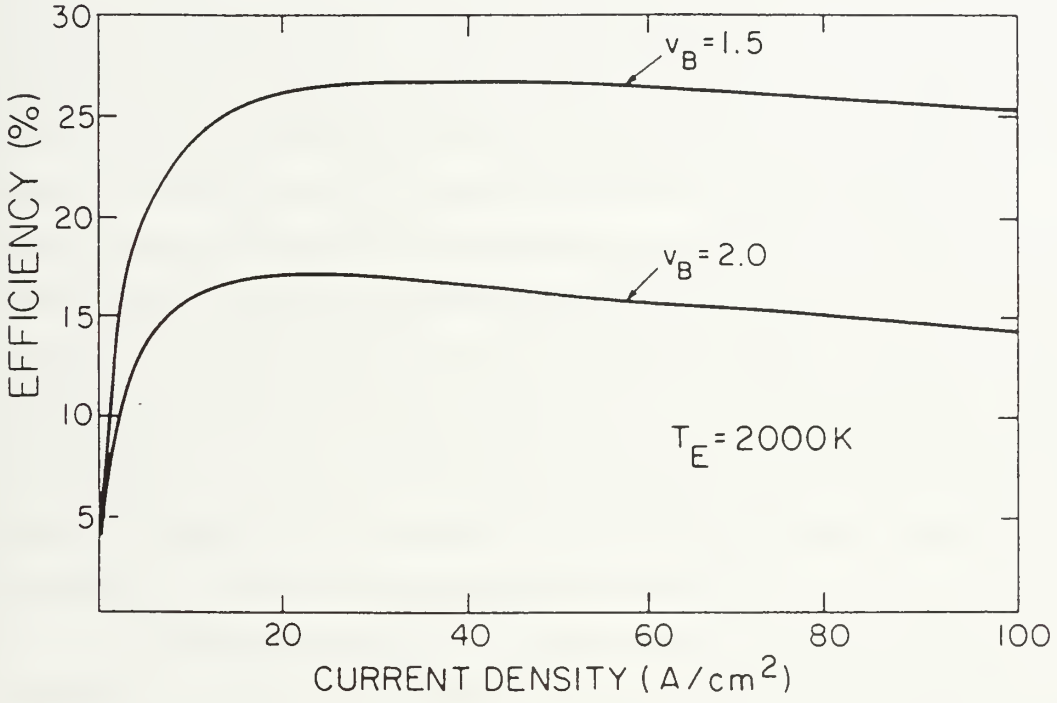

Figure 2-10. The Effect of the Space-Charge-Barrier. From (Culp, 1979).

III. RADIOISOTOPE THERMOELECTRIC GENERATORS (RTG)

A. BACKGROUND

The use of a Radioisotope Thermoelectric Generators (RTG's) by the United States as space power system was first accomplished by the Navy's Transit satellite in 1961. Since then, RTG technology has been proven to be an effective, reliable, and safe method of providing power for a wide scope of space applications. These missions include the planetary exploration of Mars, fly-bys of the outer planets, lunar scientific stations, and remote earth-sensing satellites. Some specific missions that were powered by or are to be powered by, RTG's are Nimbus, Pioneer, Viking, Transit, Apollo, Voyager, Galileo, and Cassini. The two significant capabilities of RTG systems are their ability to operate at designed parameters independent of solar radiation flux and their reliability in hostile environments of high radiation and extreme temperatures (Angelo and Buden, 1985). These advantages solve many of the engineering problems associated with designing a power system for a deep space exploration mission. The reliability and resilience of an RTG are due its simplicity. A decaying radioisotope provides heat to a thermoelectric conversion device which produces electricity.

In 1955, the Atomic Energy Commission's began the System for Nuclear Auxiliary Power Program, called SNAP. The program was to develop a family of power systems, specifically for space missions and consisted of two divisions. The first was concerned with development of radioisotope power systems, the second division's responsibility was to developed nuclear reactors for space applications. The goal of the radioisotope power unit program was to design power systems that would provide self-contained sources of power with high energy densities. The lifetime of the rugged systems was to be determined, primarily, by the half-life of the fueling radioisotope. The attainable range of power was estimated to be between 1 and 500 watts. (Pedersen, 1964)

The SNAP-3B RTG system on the Navy's Transit navigation satellite in 1961 had a mass of only 2.1 kilograms and produced 2.7 watts of electricity. Figure 3.1 is an illustration of this power system. In 1963, Transit navigation satellites required 36 watts from the SNAP-9A. In 1969, the Nimbus satellite was launched to study the earth's cloud cover from space. Its SNAP-19 produced 56 watts. Power requirements have grown steadily ever since.

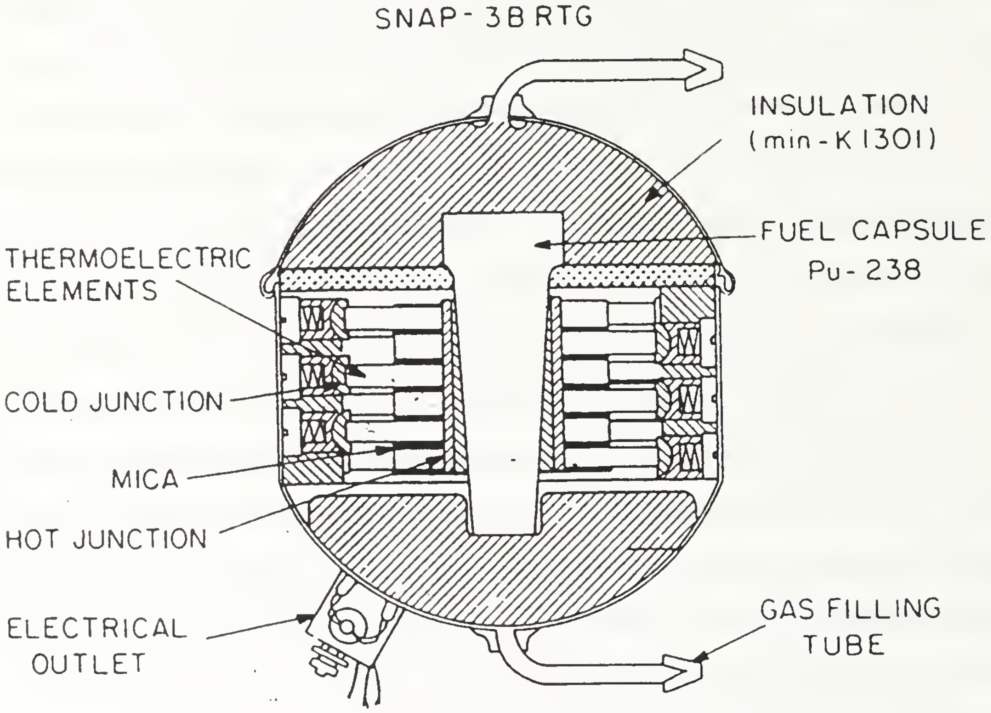
SNAP-3B RTG
INSULATION (min-K 1301)
FUEL CAPSULE Pu-238
THERMOELECTRIC ELEMENTS
COLD JUNCTION
MICA
HOT JUNCTION
ELECTRICAL OUTLET
GAS FILLING TUBE
W

Figure 3-1. The SNAP-3B RTG. From (Angelo and Buden, 1985).

The Apollo lunar missions proved that RTG systems could provide safe and reliable power to manned spacecraft with SNAP-27. Pioneer carried four SNAP-19 units to transit through the asteroid belt and explore the radiation belts around Jupiter. The Viking mission explored the surface of Mars with two landers also powered by SNAP-19 systems. Advancement to the next level of power generation was accomplished by the Multi-Hundred Watt RTG (MHW) unit. In 1977, approximately 15 years after the launch of the SNAP-3B, the Voyager exploration spacecrafts were launched with three MHW

RTG's, each generating 150 watts of electricity with only 37.6 kilograms of mass. (Angelo and Buden, 1985)

B. RTG DESIGN

The two primary components of an RTG system are the heat source and the thermal-electric conversion device. Historically, the design of these power systems has been driven by nuclear safety philosophy. Changes in this philosophy over the years have directly resulted in changes to RTG system design. The most significant of these changes concerns the event of spacecraft reentry. Early systems, such as, SNAP-3B and SNAP-9A were designed to burn up and disperse their radioisotope fuel at high altitude during reentry. In later RTG design, the radioisotope fuel is encased in a hard capsule, capable of withstanding the temperatures of reentry and the forces of impact with the earth's surface. These capsules are constructed of wound graphite fiber. The primary safety concern ion that has influenced the design of current RTG systems as well as earlier ones, is the immobilization of the radioisotope fuel during all mission phases. This means preventing fuel from interacting with the environment. If a spacecraft reenters, burning the fuel in the atmosphere or physically containing it through impact are two methods of accomplish this task. (Angelo and Buden, 1985)

1. Isotopic Fuel

The principle subsystem of the RTG power system design is the fuel. Heat from a decaying radioisotope fuels the thermal to electrical converter of an RTG. The type of radioisotope chosen as a fuel will effect performance parameters of the system such as, operating temperature and efficiency. Different radioisotopes emit different types of radiation. Radioisotopes that emit alpha particles or beta particle yield large amounts of heat. Alpha emitters are more desirable than beta emitters because the latter release bremstrahlung radiation in addition to the beta particles (Pedersen, 1964). Protecting other spacecraft components from this high energy radiation requires very heavy and expensive shielding material. Alpha emitters are preferable because they can be shielded by materials constructed of boron compounds and aluminum. They also produce more thermal energy than beta emitters. The simplicity of shielding an isotope aids in the overall optimization of the system mass. This is important to the balancing of system weight, power density, fuel availability, cost, and radiation tolerance (Pedersen, 1964). The primary unattractive feature of alpha emitters is their tendency to create high pressures inside the fuel capsule due to the generation of helium gas. Selective or non-selective vents must be used to account for this effect. Selective vents allow for the passage of helium gas molecules, but not the larger molecules of other gases and solid fuel particles. Non-selective vents prevent the escape of fuel particle but allow the passage of helium and other gaseous molecules including other decay products such as radon.

All RTG's to date have flown using Plutonium-238 as fuel. Alternatives have been studied for various programs but have not been selected for space missions. The SNAP-1 and SNAP-1A were Air Force programs that used Cesium-144. Both were canceled prior to 1960. SNAP-11, fueled by Curium-242, was designed to power the Surveyor lunar lander but this RTG was canceled in 1965. The SNAP-13 was fueled by Strontium-90 and completed a course of design and component testing in 1965. The SNAP-19A system producing 1500 watts of electricity for proposed Extended Apollo missions was fueled by Polonium-210 and underwent feasibility and design studies that ended in 1964. A similar SNAP-29 study was canceled in 1969. Plutonium-238 was chosen to be the primary RTG fuel source for its relative abundance and long life. (Angelo and Buden, 1985)

2. Energy Conversion

Another important design parameter is energy conversion efficiency. This is the ratio of output electrical power to the heat generated by the heat source. Currently, efficiencies of 5-10% are considered attainable, which limits the generation of electricity by an RTG system to about 500 watts (Pedersen, 1964). Early RTG's used lead telluride thermoelectric converters. Haynes-25, a super alloy, was used to construct fuel capsules because it could withstand the temperatures of normal operations but would burn up in the heat of atmospheric reentry. Later, the increasing temperatures of operation of germanium silicide converters required the use of noble metals and refractory alloys to contain the radioisotope fuel during normal operation. The change to these materials was was also necessitated by the requirement for the fuel container to remain intact during reentry. Current system operating temperatures have reached 1675 K and require the use of iridium alloys in the manufacturing of fuel capsules to contain the radioisotope fuel under all conditions (Angelo and Buden, 1985). Power output must be optimized as a function of the hot and cold junctions of the thermalelectric converter. The size of the elements of the converter is highly important. The temperature of the hot junction is determined by the heat generating source. The cold junction of the converter must absorb thermal energy flowing from the hot junction and reject the excess, by radiation. Selecting the proper dimensions of the radiator is critical to minimizing the cold junction temperature and thereby maximizing the efficiency of the converter. (Pedersen, 1964)

C. SNAP-3

In June of 1961, the Transit 4A navigation satellite, powered by solar arrays and SNAP-3B RTG's used nuclear power in space for the first time. Naturally, safety was of paramount concern. The two Transit satellites launched that year were placed into orbits with 1000 year lifetimes. The RTG's on board were designed to burn up and disperse, at high altitude, should the spacecraft reenter the atmosphere. (Angelo and Buden, 1985)

The original SNAP-3 design was fueled by Polonium-210 encapsulated in two, stainless steel, cylindrical containers and closely fitted into a third stainless steel canister which was surrounded by a flame-coated, non-oxidizing molybdenum core. The canisters were heliarc welded with 100% penetration. The molybdenum core was tapered to provide good contact with the hot junction of the thermoelectric converter. Elements of lead telluride were arranged radially about this heat source to form 27 thermocouples each providing a path for heat flow from the hot junction through to the cold junction. Excess heat passed through the cold junction to the outer casing, which also served as the radiator. (Pedersen, 1964)

The SNAP-3B was similarly constructed, but was fueled by 92.7 grams of Plutonium-238. Including other isotopes present, Pu-239 (16%) and Pu-240 (3%), the heat source mass totaled 359 grams. The tapered cylinder was constructed of Haynes 25 alloy for strength and lined with tantalum to provide a compatibility barrier between the plutonium and the cylinder. The heat source produced 52.5 watts of thermal energy at 810 K. The converter produced 2.7 watts-electrical at an overall system efficiency of 5%. Lead telluride was used in the thermal electric converters. Contact between the hot and cold junctions was made by springs and the energy conversion efficiency of the system was 5%. The SNAP-3B had a design life of less than one year. Two Transit-4A satellites were launched in 1961. The generator launched in June functioned until 1976 and the one launched in November functioned until 1971, greatly exceeding design expectations. (Angelo and Buden, 1985)

D. SNAP-9A

The follow-on to the SNAP-3B was designed to power the Transit 5 satellites. Solar cells were deemed to be an unfavorable option for this mission due to the degradation they would suffer as the result of exposure to Van Allen belt radiation. It was estimated that significant reduction in cell output would result when the radiation dose reached 5e13 electrons per square centimeter. The estimated dosage for the planned five to six year mission was 1e15 electrons per square centimeter. The use of heavy filters was considered as a means to prolong the life of a solar array, however, such filters degrade with time. (Pedersen, 1964)

The SNAP-9A utilized six isotopic heat sources to supply 25 watts of electrical power. Again, a tantalum lined Haynes 25 alloy capsule contained each 458 gram heat source. Solid plutonium metal fuel was used in SNAP-3B. During the construction of the SNAP-9A, each fuel capsule was heated to 890 K. This caused the plutonium-238 to melt. When it cooled, the metal bonded itself to the lining of the capsule improving heat transfer during operation. A graphite block was used to both hold the capsules in place and to conduct heat to the thermoelectric converters. An illustration of a SNAP-9A fuel capsule is provided in Figure 3-2. (Angelo and Buden, 1985)

As was the case in previous RTG's, SNAP-9A was designed to burn up and disperse in the event of atmospheric reentry due to mission abort. The graphite block which housed the fuel capsule was segmented to allow the containers to be exposed to the heat of atmospheric reentry. The Haynes 25 material of the capsules was designed to melt at this reentry temperature, however it would resist corrosion in a marine environment. This resulted in system that would "burn up and disperse" during atmospheric reentry, but contain the radioisotope in the event of a launch abort prior to reaching orbit.

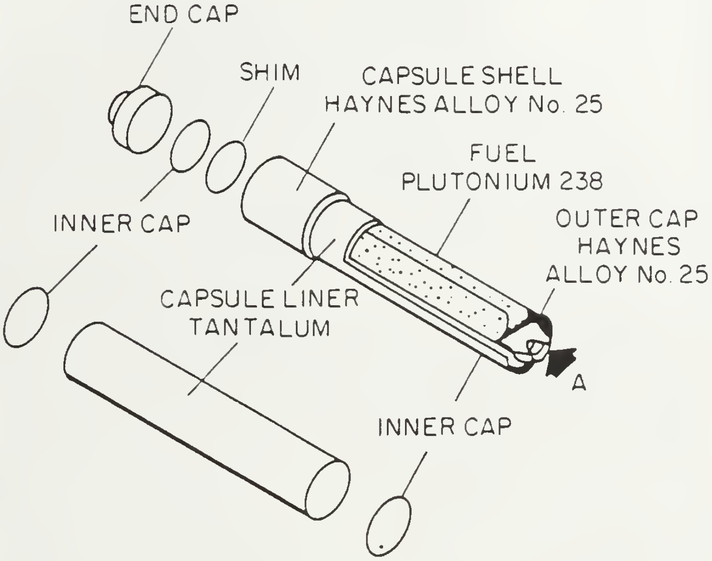
END CAP
SHIM
CAPSULE SHELL
HAYNES ALLOY No. 25
FUEL
PLUTONIUM 238
INNER CAP
OUTER CAP
HAYNES
ALLOY No. 25
CAPSULE LINER
TANTALUM
A
INNER CAP

Figure 3-2. The SNAP-9A RTG. From (Angelo and Buden, 1985).

E. SNAP-19

The SNAP-19 RTG powered the Nimbus 3 meteorological satellite. Its first successful launch was in April of 1969. This generator introduced the Intact Impact Heat Source, fueled by plutonium-238 and producing 645 watts of thermal energy. The thermoelectric converter unit was made up of 90 lead telluride and silver antimony germanium telluride thermocouples (Angelo and Buden, 1985). This design marked a change in aerospace nuclear safety policy. Under all conditions, the fuel encapsulation system of this RTG was to contain the radioisotopic heat source, to include the events of atmospheric reentry and impact. Figure 3-3 is an illustration of the SNAP-19 RTG.

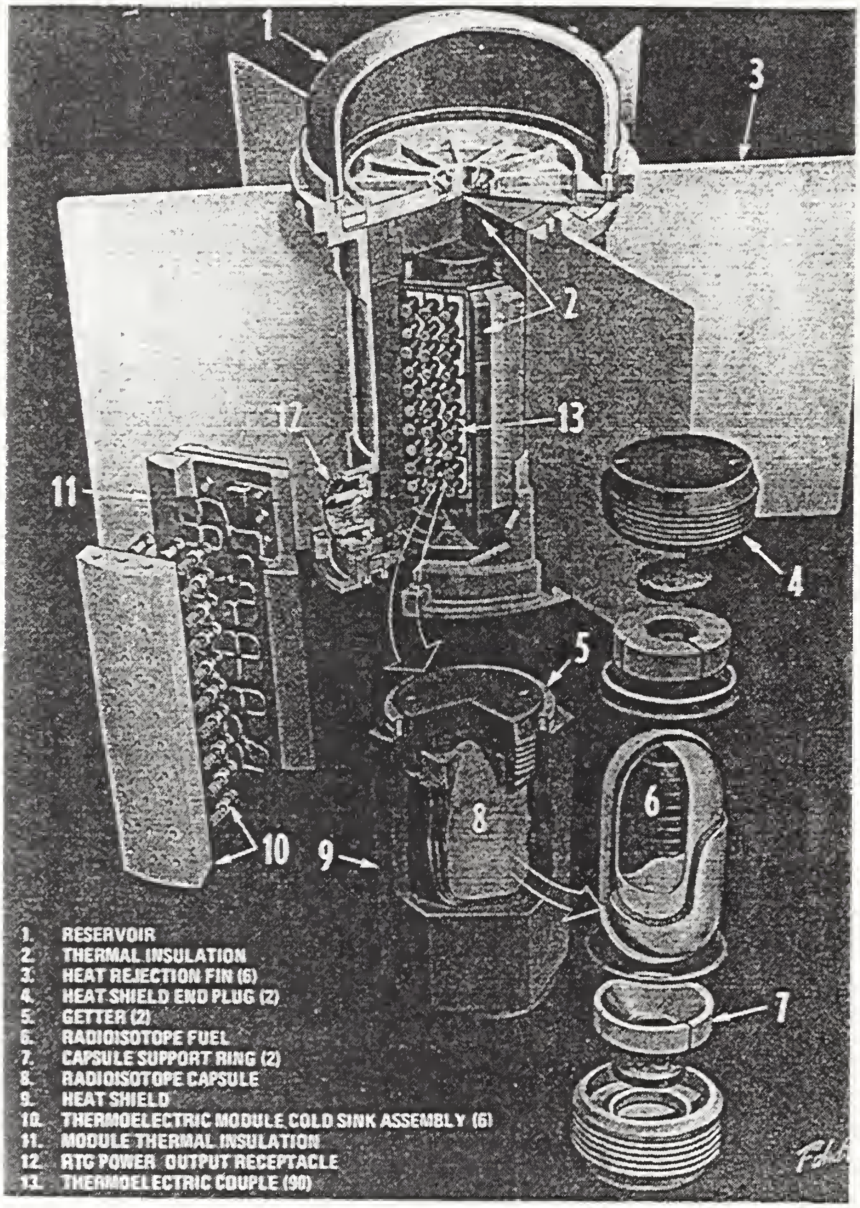
1
2
3
4
5
6
7
8
9
10
11
12
13
1. RESERVOIR
2. THERMAL INSULATION
3. HEAT REJECTION FIN (6)
4. HEAT SHIELD END PLUG (2)
5. GETTER (2)
6. RADIOISOTOPE FUEL
7. CAPSULE SUPPORT RING (2)
8. RADIOISOTOPE CAPSULE
9. HEAT SHIELD
10. THERMOELECTRIC MODULE COLD SINK ASSEMBLY (6)
11. MODULE THERMAL INSULATION
12. RTG POWER OUTPUT RECEPTACLE
13. THERMOELECTRIC COUPLE (90)

Figure 3-3. The SNAP-19 RTG. From (Angelo and Buden, 1985).

On Nimbus 3, SNAP-19 functioned for more than two times its design life and then suffered a relatively sudden reduction in performance caused by a loss of contact between the heat source and the hot junction of the thermoelectric converter. The design was corrected and the design life was increased to six years which provided power for the Pioneer missions to Jupiter and Saturn and the Viking missions to Mars. Pioneer 10 was launched in 1972, followed by Pioneer 11 in 1973. The power systems of both spacecraft have exceeded their design lives. Pioneer 10 became the first spacecraft to travel beyond the bounds of our solar system in 1983. Vikings 1 and 2 were launched in 1975 and traveled to Mars. In 1976 both spacecraft orbited Mars and successfully landed robotic explorers on the Martian surface. Unique aspects of these planetary exploration missions called for modifications to the SNAP-19 design. The Viking SNAP-19 heat source was constructed of 18 or 19 plutonium-238 dioxide-molybdenum cermet discs arranged in a layered tantalum cylinder which was encased in a hexagonally-shaped graphite shield. This design met the safety requirements of intact reentry and impact and produced 682 watts of thermal energy. The fuel discs were separated from the other components by a molybdenum-46% rhenium oxygen barrier. The fuel was encapsulated primarily by a tantalum-10% tungsten liner. The gases generated by decay of the isotope were vented by a pressure relief valve. A tantalum alloy shell hardened the fuel capsule against impact and an outer shell of platinum-20% rhodium provided an outer oxygen barrier. A platinized aluminum coating increased the emissivity of the outer shell facilitating heat transfer to the graphite shield which provided the ablative properties that would be needed in the event of reentry. The graphite heat shield functioned as the heat sink during normal system operations. This summarizes but does not exhaust the list of structural and electrical modifications made to the earlier SNAP-19 design. The thermoelectric converter consisted of 15 thermocouples of SnTe and PbTe materials. The magnesium-thorium outer cylindrical housing employed a configuration of six fins and ribbed end caps for heat rejection. The earlier problem of losing contact between the heat source and the hot junctions was corrected by adding a reservoir of argon gas. This slowed sublimation of the thermoelectric converter materials during operation (Angelo and

Buden, 1985). Very significant advances in materials and converter design were made to accomplish the longer, more demanding missions of Viking and Pioneer.

F. SNAP-27

The Apollo Program introduced a new set of system requirements and challenges. The SNAP-27 was designed to power instrument and experiment packages to be left on the surface of the moon. This was also the first space mission in which man was to fly with RTG's. The SNAP-27's major hardware components included a generator with a thermopile structure and heat rejection system, a hermetically sealed plutonium fuel capsule, and a graphite lunar module fuel cask. The fuel capsule, shown in Figure 3-4, and the cask were engineered to provide support for the fuel module as well as thermal and blast shielding in the event of a mishap. The specific mishaps accounted for in the design were, launch pad explosion, ascent abort, atmospheric reentry, and ground impact.

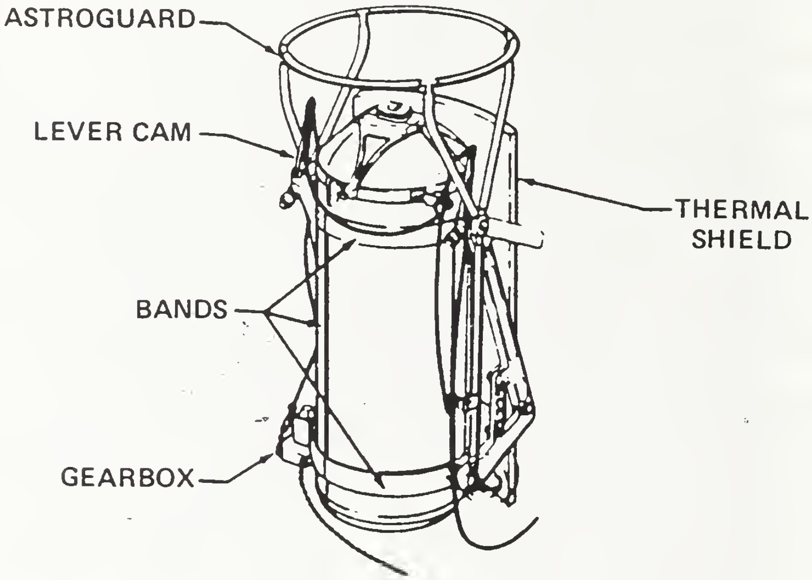

Figure 3-4. SNAP-27 Fuel Capsule. From (Angelo and Buden, 1985).

The capsule construction incorporated two fuel compartments enclosed by a Haynes super alloy each compartment producing 748 watts of thermal energy. The fuel was in the form of plutonium-238 dioxide microspheres. The fuel compartments utilized an annular configuration to provide space for the generation of helium gas during mission life. The cask was designed to hold the fuel capsule in place. The cylindrical cask was constructed of graphite with hemispherical end caps. A secondary heat shield was constructed of beryllium with high emissivity coatings. During operation, energy from the heat source was radiated to the generator hot frame. Thermal energy passed from the hot frame through an insulator to the electrode at the hot side of the thermoelectric converter. The hot junction was designed to operate over the range between 855 and 865 K. This range resulted from the differing temperatures of lunar day and night which are 350 K and 100 K, respectively. The converter utilized lead telluride material and incorporated insulation to reduce heat loss. Figure 3-5 illustrates the complete SNAP-27 configuration (Angelo and Buden, 1985). Table 3-1 summarizes the design characteristics of the SNAP RTG's.

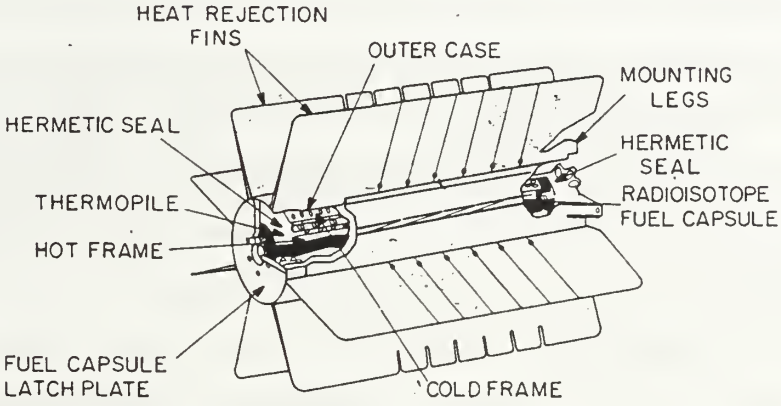

Figure 3-5. SNAP-27 RTG. From (Angelo and Buden, 1985).

G. TRANSIT-RTG

Specifically designed for navigation satellites, the Transit-RTG met the mission requirements of 34.2 watts of electrical power for a 5 year life. A problem associated with high operating temperatures of an RTG is the sublimation of thermocouple material, primarily at the hot junction. Some previous RTG designs utilized argon gas, injected into the compartment housing the thermocouples, to retard this effect. The Transit system was simpler in that it did not use a this cover gas method. The heat source did not make physical contact with the hot junction of the thermocouples. It was the first RTG to rely upon the radiative heat transfer of thermal energy between the radioisotope heat source and thermoelectric converter. In this case, the simpler design resulted in a reduction of overall system efficiency.

This generator had two primary components, the heat source and the thermoelectric converter. Figure 3-6 provides an illustration of the Transit thermoelectric converter. Like the Viking SNAP-19, plutonium-238 dioxide molybdenum cermet discs were the selected fuel configuration. Two of these discs produced 850 watts of thermal energy from approximately 2.64 kilograms of fuel. The fuel was contained in a three-layered refractory metal capsule and enclosed by a two-layer graphite heat shield to provide thermal protection during reentry as well as reduce impact velocity. An outer can protected against oxidation during storage, prior to launch. The thermoelectric converters were shaped as panels and formed a 12-sided prism. Instead of cover gas to reduce sublimation of the converter components, quartz washers were used to prevent shunting between the hot junction, the cold junction, and the insulation materials. (Angelo and Buden, 1985)

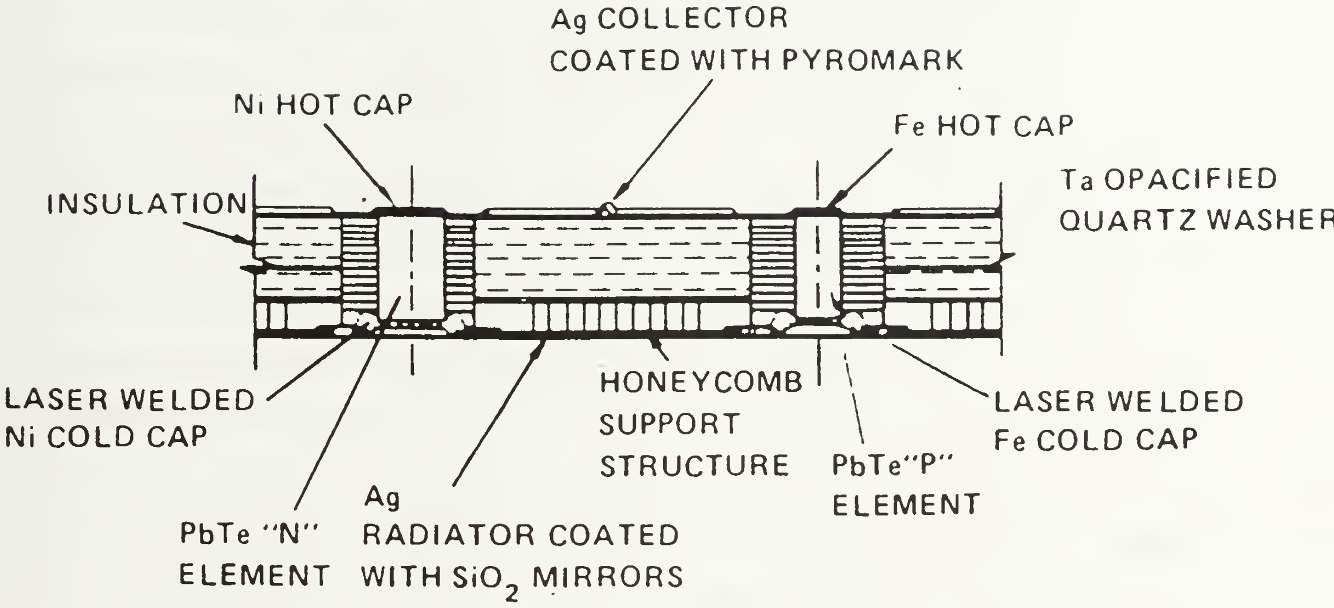
Ag COLLECTOR
COATED WITH PYROMARK
Ni HOT CAP
Fe HOT CAP
Ta OPACIFIED
QUARTZ WASHER
INSULATION
LASER WELDED
Ni COLD CAP
HONEYCOMB
SUPPORT
STRUCTURE
LASER WELDED
Fe COLD CAP
PbTe"P"
ELEMENT
Ag
RADIATOR COATED
WITH SiO_2 MIRRORS
PbTe "N"
ELEMENT

Figure 3-6. Transit Thermoelectric Converter. From (Angelo and Buden, 1985).

	SNAP-3B	SNAP-9A	SNAP-19	SNAP-27	Transit-RTG	MHW	GPHS-RTG
Mission	Transit	Transit	Nimbus Pioneer Viking	Apollo	Transit	LES 8/9 Voyager	Galileo
Fuel form	Pu metal	Pu metal	PuO_2-Mo cermet	PuO_2 microspheres	PuO_2-Mo cermet	Pressed PuO_2	Pressed PuO_2
Thermoelectric material	PbTe	PbTe	PbTe-TAGS	PbSnTe	PbTe	SiGe	SiGe
BOL[1] output power (W_e)	2.7	26.8	28–43	63.5	36.8	150	290
Mass (kg)	2.1	12.2	13.6	30.8[2]	13.5	38.5	54.4
Specific power (W_e/kg)	1.3	2.2	2.1–3.0	3.2[3]	2.6	4.2	5.2
Conversion efficiency (%)	5.1	5.1	4.5–6.2	5.0	4.2	6.6	6.6
BOL fuel inventory (W_{th})	52	565	645	1480	850	2400	~4400
Fuel quantity (curies)	1800	17,000	34,400 – 80,000	44,500	25,500	7.7×10^4	1.3×10^5

[1] BOL = beginning of life
[2] without cask
[3] includes 11 1-kg cask

Table 3-1. SNAP RTG Parameters. From (Angelo and Buden, 1985).

H. MULTI-HUNDRED WATT (MHW) GENERATOR

The Multi-hundred Watt generator was designed to produce 150 watts of electricity at an efficiency of 6.7%. The Lincoln experimental communication satellites, LES-8 and LES-9, were each powered by two MHW's and launched in 1976. Three of these RTG's were used to power each of the two Voyager spacecraft that were launched in 1977 to conduct flyby missions of the outer planets and continue beyond the solar system.

As defined by aerospace nuclear safety philosophy, the priorities of the design were to prohibit the release of nuclear fuel, minimize contamination of the biospheric environment, and optimize immobilization in the event of a heat source accident. The generator was made up of two major components, the heat source and the energy converter. The fuel was contained in the form of spherical balls of plutonium dioxide each with an iridium shell. Each shell contained 6.05 kilograms of fuel. An added shell of graphite protected against impact. The cylindrical heat source contained 24 of these fuel capsules and generated 2400 watts of thermal energy. Figure 3-7 illustrates the MHW's heat source. Ablative protection during reentry was provided by a secondary, aerodynamic shell of graphite. The MHW RTG utilized a heat source that operated at 1330 K, a higher temperature than previous designs. To accommodate this, germanium silicide materials were used in the thermal electric converter of the system. The fuel capsules were configured in six planes, each housing four of the spheres. The outer core of the converter was made of beryllium and couples were attached directly to it within a pressure dome. The outer shell was coated with iron-titanate to serve as a highly emissive surface for converter heat rejection. There were a total of 312 SiGe thermocouples arranged circumferentially around the core. Energy from the heat source radiated through each thermocouple through means of a SiMo hot shoe. The other end of the thermocouple was bonded to a cold stack constructed of tungsten, copper, and alumina. Sublimation of the thermocouple materials was reduced by a layer of silicon nitride. The hot and cold shoes were insulated against heat loss by layers of molybdenum foil and Astroquartz. (Angelo and Buden, 1985)

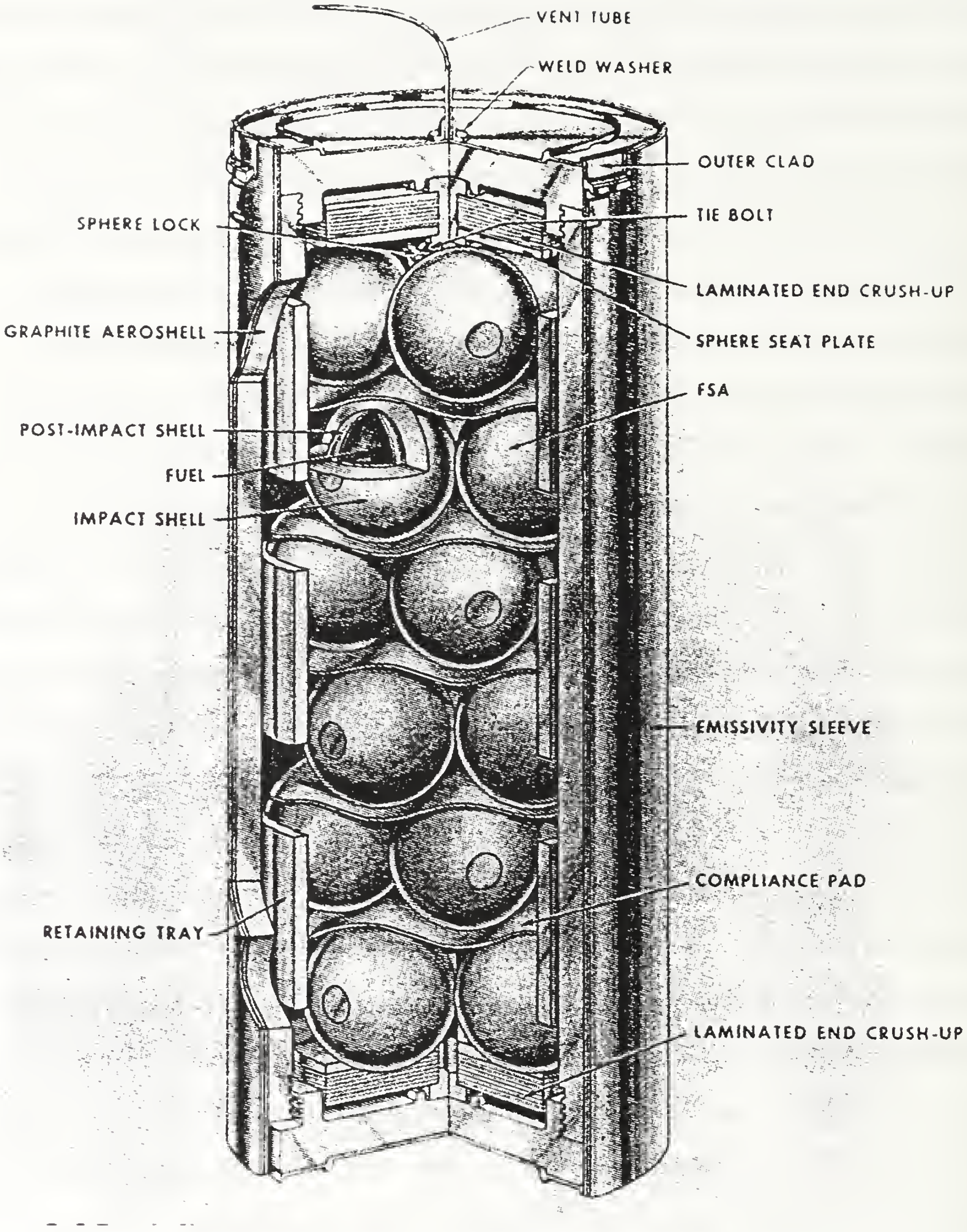
VENT TUBE
WELD WASHER
OUTER CLAD
SPHERE LOCK
TIE BOLT
LAMINATED END CRUSH-UP
GRAPHITE AEROSHELL
SPHERE SEAT PLATE
FSA
POST-IMPACT SHELL
FUEL
IMPACT SHELL
EMISSIVITY SLEEVE
COMPLIANCE PAD
RETAINING TRAY
LAMINATED END CRUSH-UP

Figure 3-7. MHW RTG Heat Source. From (Angelo and Buden, 1985).

I. GENERAL PURPOSE HEAT SOURCE (GPHS)

The GPHS RTG introduced a new concept in generator design by supporting missions of increasing power requirements by providing a modular power system that could be sized by selecting the number of heat sources and energy converters to suit specific needs. The result was a generator system that could be adapted to a spacecraft in increments of 250 watts-thermal. Galileo and Cassini utilize GPHS. Figure 3-8 illustrates the GPHS RTG configuration.

As before, the design of GPHS was centered around the containment of the radioisotopic fuel under the potential conditions of atmospheric reentry, launch orbit, and impact. In a GPHS generator system, individual fuel modules are stacked. Each module is encased in an aerodynamic shell and two graphite impact shells. Each module has a vent hole to release the helium gas generated by isotope decay during operation while containing particulates. The stacked modules are held in place by structural members. The same thermal converter used in the MHW RTG is also used in the GPHS system. The heat source is surrounded by 576 germanium silicide thermocouples. The thermocouples and the heat source are supported by an outer case which also provides heat rejection. The support system is preloaded to withstand the g-forces of launch then to hold the heat source in place during operation. The converter component provides multi-layered foil insulation and a gas management system. An inert gas is used during storage to protect the molybdenum foil insulation and refractory materials. The outer case of the system must be actively cooled until the space craft is deployed. (Angelo and Buden, 1985)

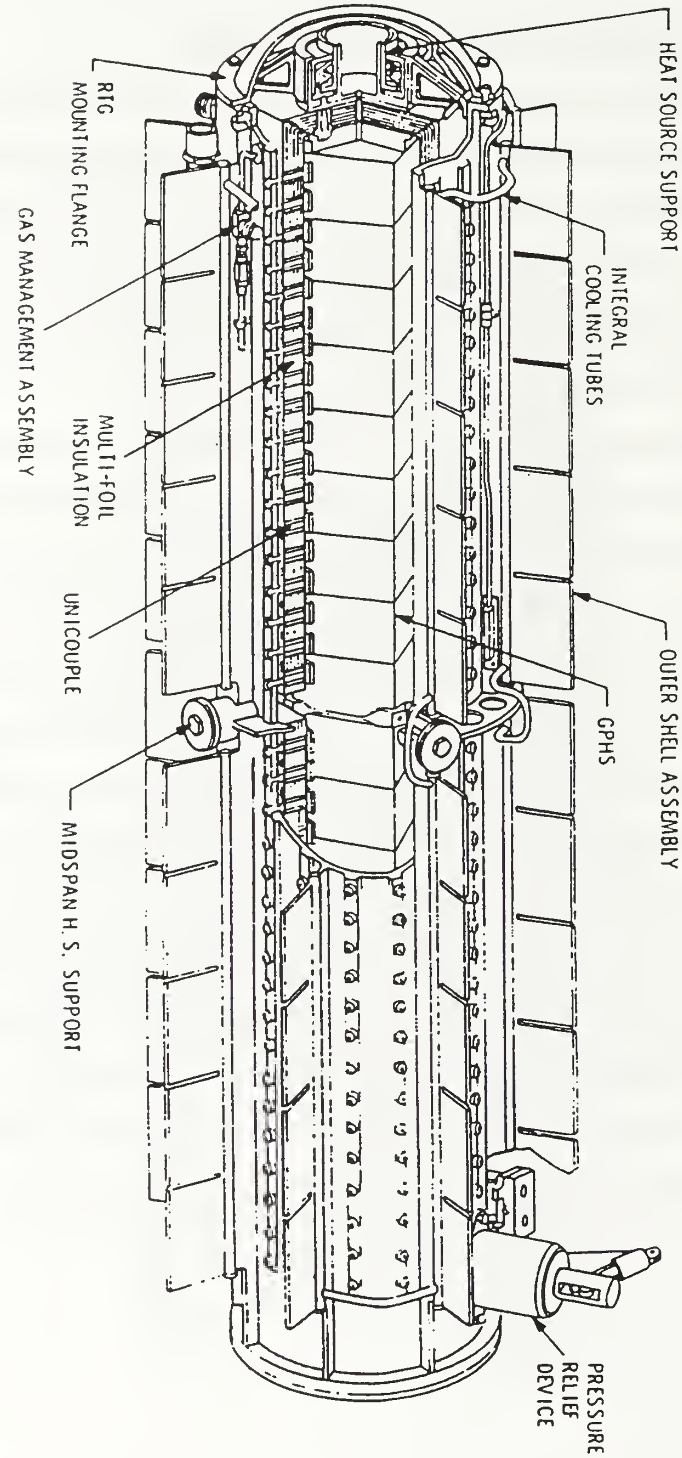
HEAT SOURCE SUPPORT
RTG MOUNTING FLANGE
GAS MANAGEMENT ASSEMBLY
INTEGRAL COOLING TUBES
MULTI-FOIL INSULATION
UNICOUPLE
OUTER SHELL ASSEMBLY
GPHS
MIDSPAN H. S. SUPPORT
PRESSURE RELIEF DEVICE

Figure 3-8. GPHS RTG. From (Angelo and Buden, 1985).

IV. SPACE NUCLEAR REACTORS

A. BACKGROUND

Nuclear reactors for space provide the greatest promise for the generation of the power levels required for missions such as, the manned exploration of Mars and the establishment of a permanent lunar base. Recall that RTG's generate electricity from the heat of a decaying radioisotope while reactor systems generate electricity from the heat of controlled nuclear fission reactions. The growing need for power was recognized early in the history of space exploration. Between 1955 and 1973, the United States pursued the development of nuclear reactors for space missions through the efforts of the Nuclear Rocket Program (Project Rover) and the Systems for Nuclear Auxiliary Program (SNAP).

Initial efforts to develop a nuclear reactor for space in the United States were a part of the joint Atomic Energy Commission-Air Force-NASA Project Rover, which began in 1955. The goal of this project was to research and develop the technologies necessary to build a nuclear rocket and encompassed the many systems necessary to support nuclear space propulsion. The rocket was called, the Nuclear Engine for Rocket Vehicle Application (NERVA). In this system, heat was provided to a nuclear rocket by a nuclear reactor. Reactor development was only a portion of the Nuclear Rocket Program. The reactors developed by this program were fueled by uranium-235 and their function was to provide thermal energy to heat the hydrogen fuel used in the operation of a rocket engine. The use of a fraction of this energy to provide electrical power to a spacecraft was explored in by the dual-mode reactor concept. Prior to the flight of NERVA, funding for the nuclear rocket program was terminated in 1972.

The Atomic Energy Commission's program for the development of Systems for Nuclear Auxiliary Power Program, known as SNAP, began an effort to build space nuclear reactors in 1957. The SNAP reactors developed the use of uranium-zirconium-hydride as a fuel and were specifically designed to generate electricity for space missions. All of the SNAP reactor programs were terminated by the end of 1972.

B. NUCLEAR ROCKET PROGRAM REACTORS

The first nuclear reactor experiments under this program were called Kiwi-A and were conducted in 1959. Kiwi-A succeeded, although it was never intended for space launch. The project was a series of three reactors built to test the operation of a nuclear reactor at a controlled temperature for the duration of a typical mission. Uranium-235 and graphite provided fuel and the coolant was gaseous hydrogen. The next series, Kiwi-B, demonstrated the use of liquid hydrogen as a coolant and propellant. Kiwi-B was subjected to flight stresses on a test stand. Figure 4-1 illustrates the Kiwi reactor design.

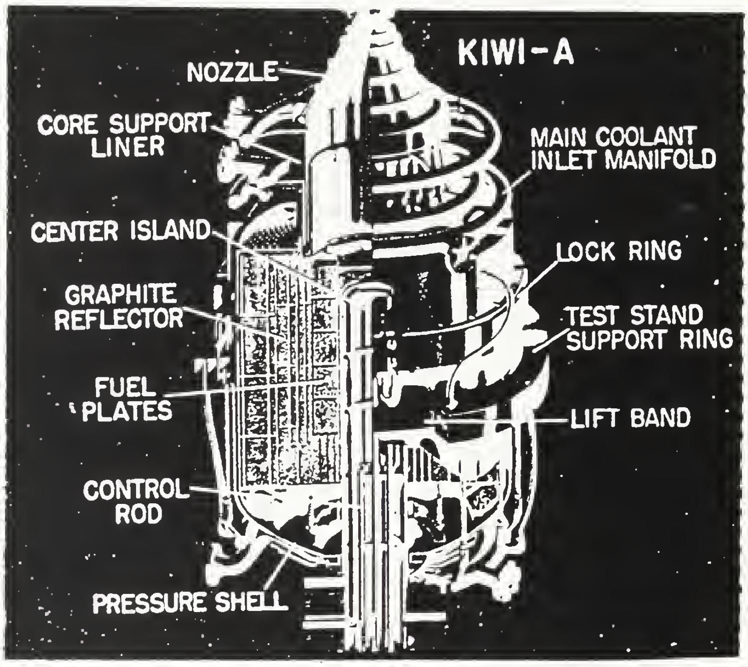
KIWI-A
NOZZLE
CORE SUPPORT LINER
CENTER ISLAND
GRAPHITE REFLECTOR
FUEL PLATES
CONTROL ROD
PRESSURE SHELL
MAIN COOLANT INLET MANIFOLD
LOCK RING
TEST STAND SUPPORT RING
LIFT BAND

Figure 4-1. The Kiwi-A Reactor. From (Pedersen, 1964).

The Kiwi series was followed by the NRX test reactors. Then, a Kiwi-type reactor series capable of greater power output, called Phoebus, was built to increase the specific impulse of a rockets. Pewee and Nuclear Furnace experimented with high temperature fuel sources with longer lives. The NRX and XE series reactors were the first tests of the NERVA design, which was to be built and flown sometime between 1968 and 1969. At the time, NASA had planned to acquire some 30-40 NERVA's to be used to replace various stages of the Saturn chemical rocket booster. (Pedersen, 1964)

The reactors designed and built as a part of Project Rover were successful in many ways. The primary goals of the program were to develop reactors that would provide the greatest propellant exit temperature, operate for a duration of 10 hours, and minimize fuel corrosion and breakage.

The Kiwi-B4E was the final reactor of the series. It overcame vibrational problems that had been present since early in the program. It operated at 2005 K and produced 937 megawatts for a duration of 95 seconds. The NRX-A6 generated 1100 megawatts at 2220 K for 62 minutes. In June 1968, the Phoebus-2A reactor became the most powerful of the space nuclear reactors. It surpassed the thermal power output of all other space reactors, producing 4000 megawatts for 12 minutes.

C. SNAP NUCLEAR REACTORS

1. SNAP-2

The first reactor designed by this project was called SNAP-2. Development began in 1957. As the first of the uranium-zirconium-hydride reactors, SNAP-2 faced many new design challenges. Energy conversion in this reactor system was accomplished by a Rankine cycle dynamic converter that used mercury as a working fluid, shown in Figure 4-2. In a Rankine cycle energy converter, the working fluid is pumped through the nuclear reactor and heated. The thermal energy of the fluid is then used to turn turbomachinery which generates electricity. Most of the design challenges associated with this type of energy conversion pertained to containing the mercury working fluid and protecting system components from the effects of mercury corrosion.

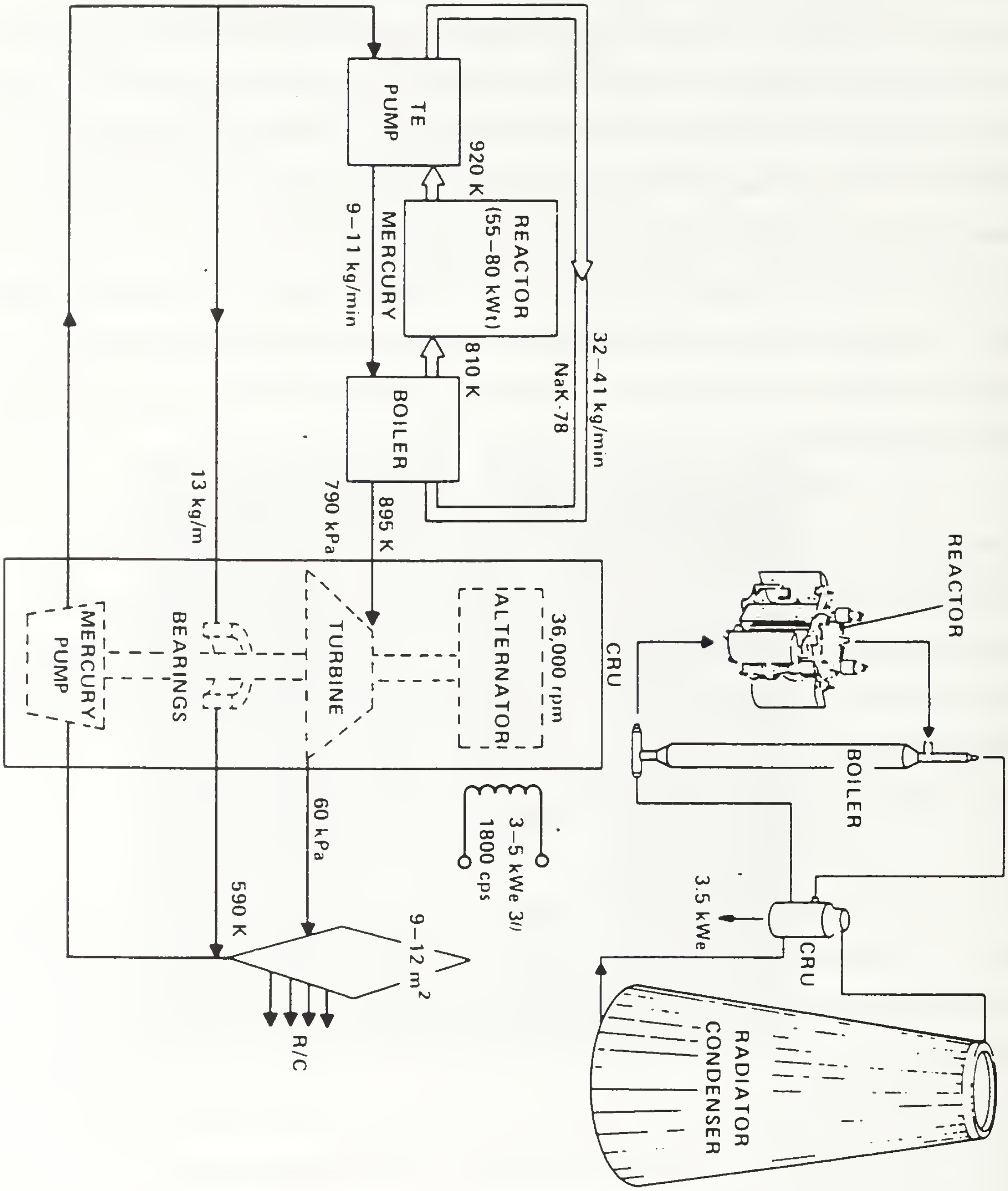

TE PUMP
920 K
REACTOR (55–80 kWt)
MERCURY
9–11 kg/min
810 K
BOILER
NaK-78
32–41 kg/min
13 kg/m
790 kPa
895 K
CRU
36,000 rpm
ALTERNATOR
TURBINE
BEARINGS
MERCURY PUMP
3–5 kWe 3Ø
1800 cps
60 kPa
590 K
9–12 m²
R/C
REACTOR
BOILER
3.5 kWe
CRU
RADIATOR CONDENSER

Figure 4-2. SNAP-2 Rankine Cycle Diagram. From (Angelo and Buden, 1985).

The high rotational speed and small tolerances of dynamic converter systems introduced other considerations, such as the erosion of turbomachinery surfaces, due to cavitation. The sodium potassium coolant (NaK-78) of the primary loop was moved through the reactor by an electromagnetic pump where it cooled the heat source. The reactor coolant also heated the mercury secondary loop as it passed through a boiler, and then returned to the reactor. In the boiler, thermal energy was transferred from the liquid metal of the primary loop to the liquid mercury of the secondary loop by means of a counterflow, single-pass heat exchanger. After leaving the boiler, the gaseous mercury was expanded through a turbine, cooled by a radiator, and then pumped back to the boiler. The turbine rotated a shaft which drove an alternator to produce electricity. An important aspect of this design was the presence of only one rotating shaft. (Angelo and Buden, 1985). The mercury pump, the impulse turbine, the permanent magnet, and the three-phase alternator, shared one shaft and were called the combined rotating unit. Minimizing the number of moving parts in the reactor design minimized the need for bearings and seals, all of which had the potential to leak mercury or wear prematurely. Innovative ideas were used to solve many problems in the design the of this space nuclear reactor. The electromagnetic (EM) pump that moved the NaK-78 through the primary loop was originally intended to be part of the combined rotating unit. This over-complicated the design and subsequently, the EM pump was powered thermoelectrically. A very small amount of heat from the primary loop was converted thermoelectrically to electricity to power the EM pump. Another complication arose from the absence of gravity in the space environment. Convective mixing could not be relied upon to aid heat transfer in the boiler. The laminar flow of coolant through the heat exchanger tubing results in boundary layers along the tube walls that reduce heat transfer. To remedy this, swirl wires were installed inside tubing to produce mixing. (Angelo and Buden, 1985)

Two versions of the SNAP-2 reactor were built over duration of the program. One of them was experimental and the other was developmental. They were called the SER and the SD2R, respectively. Both were fueled by uranium-zirconium-hydride and used beryllium reflectors and control drums to regulate reactor power output. The reactor core was made up of 37 fuel rods arranged in a hexagonal cylinder. Figure 4-3 illustrates the cross-section of the SNAP-2 reactor core. Each fuel rod was encased in a ceramic-lined, Hastelloy cylinder. Liquid metal from the primary loop passed through a plenum chamber at the lower end of the core and traveled upwards to exit at the upper end of the core. The technical issues addressed by the testing of the SER and S2DR explored the criticality of U-ZrH reactors and the fabrication of fuel elements. Development of their dynamic energy converters advanced the technologies of mercury-lubricated bearings, high rotation speed turbomachinery, and mercury corrosion resistance. The reactors also demonstrated the automated operations of a mercury Rankine system. The SER operated for 5300 hours at a power level of 50 kilowatts-thermal. The S2DR operated for 10500 hours at 57 kilowatts-thermal. The success of this program confirmed the feasibility of operating a reactor of this size for a full year in the 50 kilowatt power range. (Angelo and Buden, 1985)

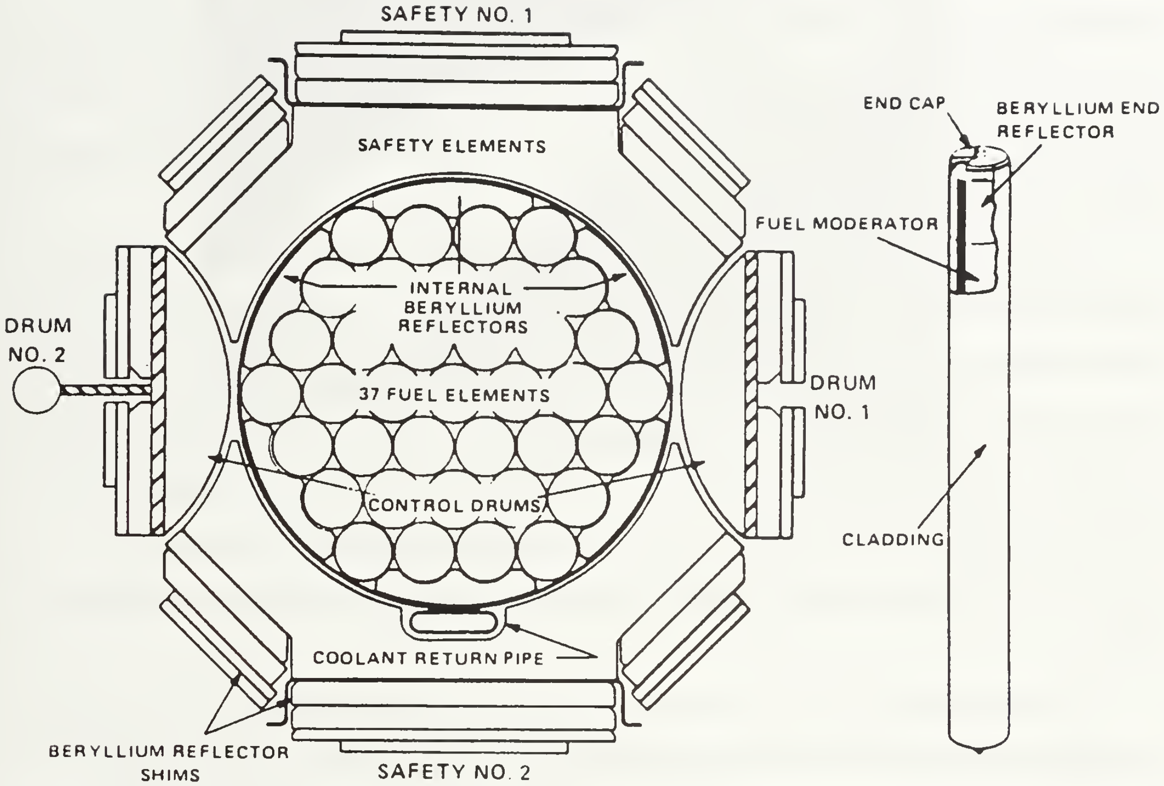
SAFETY NO. 1
SAFETY ELEMENTS
END CAP
BERYLLIUM END REFLECTOR
FUEL MODERATOR
INTERNAL BERYLLIUM REFLECTORS
DRUM NO. 2
37 FUEL ELEMENTS
DRUM NO. 1
CONTROL DRUMS
CLADDING
COOLANT RETURN PIPE
BERYLLIUM REFLECTOR SHIMS
SAFETY NO. 2

Figure 4-3. SNAP-2 Reactor Core. From (Angelo and Buden, 1985).

2. SNAP-10A

The SNAP-10A program began in 1960 with the goal of developing a reactor to generate 500 watts of electricity over a one-year life-cycle. Again, the reactor fuel was uranium-zirconium-hydride cooled by liquid metal, NaK-78. Although it was based upon the SNAP-2 design, this reactor used thermoelectric power conversion instead of a dynamic Rankine cycle system. The converter thermocouples were made of silicon germanium because this material performed better than lead telluride at temperatures above 700 K. Sodium potassium traveled through the reactor core by way of 40 separate tubes. There were 72 thermocouples positioned along the length of each tube. Excess heat was radiated into space. The reactor was to be launched into orbit and flight-tested during a mission called, SNAPSHOT.

Like its predecessor, the SNAP-10A core contained 37 fuel rods and the reactor utilized beryllium reflectors and control drums to regulate its power level. These controls were the reactor's only moving parts. A major design issue of the SNAP-10A was the minimization of shielding mass. A conical shield was designed to cast a shadow beneath the reactor. All spacecraft components were placed in the shadow of the shield. The shield was made of a lithium hydride pressed into a stainless steel honeycomb and covered by a stainless steel skin. Figure 4-4 depicts the SNAP-10A. (Angelo and Buden, 1985)

Because SNAP-10A did not become radioactive until after reaching orbit, special handling procedures prior to launch were minimal. It was mated to an Atlas-Agena launch vehicle and moved to the launching pad using normal methods. On April 3, 1965 it became the first nuclear reactor to be launched and operated in space. After 43 days, the reactor shut itself down due to a failure of a voltage regulator in the Agena space vehicle. This shutdown was not considered to be a failure of the SNAP-10A. The reactor performed fully to the expectations of its design and slightly more efficiently than predicted. None of the system components evidenced any negative effects due to the space environment. The level of radiation measured at the lower end of the Agena vehicle was lower than expected levels by a factor of two. A ground tested version of the

SNAPSHOT reactor ran successfully for 10000 hours confirming SNAP-10A's effectiveness. (Angelo and Buden, 1985)

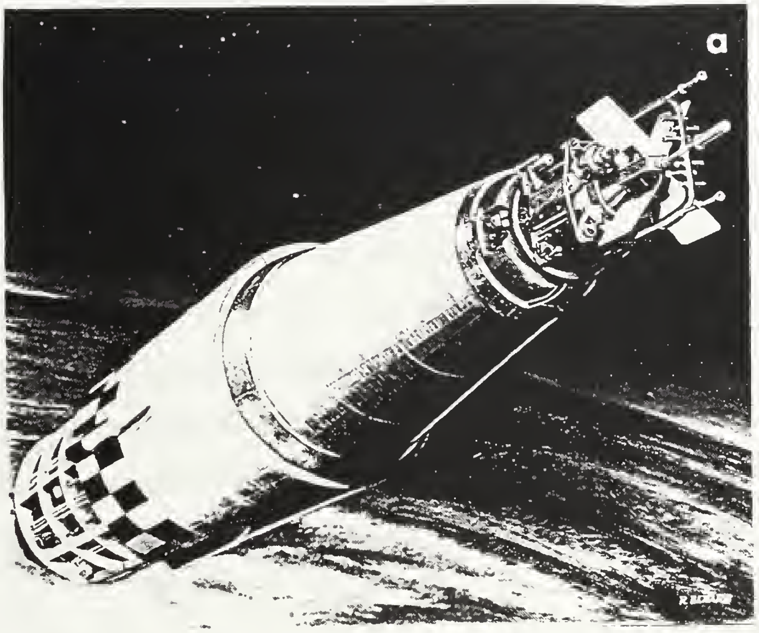

Figure 4-4. The SNAP-10A Reactor. From (Corliss, 1966).

3. SNAP-8

In 1960, development of the SNAP-8 began the with goal of designing a reactor with greater power output, 35 kilowatts. This reactor was also based upon the SNAP-2 design of uranium-zirconium-hydride fuel, liquid metal coolant, and a Rankine cycle power converter. The two reactors designed, the S8ER and the S8DR, did not utilize the combined rotating unit concept of SNAP-2. These reactors were built with four separate loops driven by individual pumps, illustrated in Figure 4-5. They were the primary loop, the mercury secondary loop, the lubricant/coolant loop, and the heat rejection loop. The lubricant/coolant loop provided lubrication for the components of the secondary loop and cooled the alternator, pumps, and electrical controls. The heat rejection loop used NaK to carry thermal energy away from the condenser to a radiator. (Angelo and Buden, 1985)

The S8ER system was tested to demonstrate dynamic stability and was subjected to a series of transients. The S8DR reactor was based upon the S8ER with some modifications to the reactor core designed to prevent cracking of the fuel element casings. Other changes improved the flow of coolant through the reactor core and improve the efficiency of the controls. The fuel elements of the S8DR still experienced some of the same cracking as the S8ER and the coolant temperatures were above design level. The alternator and pumps of the system functioned well during testing. The S8ER was operated between 400 and 600 kilowatts-thermal for more than one year. The S8DR was operated for 8300 hours at 600 kilowatts-thermal. The overall result of cracking in the fuel elements was the escape of hydrogen, significantly reducing the life of the reactor. It was determined from these experiments that uranium-zirconium-hydride reactors with power converters utilizing rotating machinery could support a mission life of five years. Table 4-1 summarizes the parameters of the SNAP reactor designs. (Angelo and Buden, 1985)

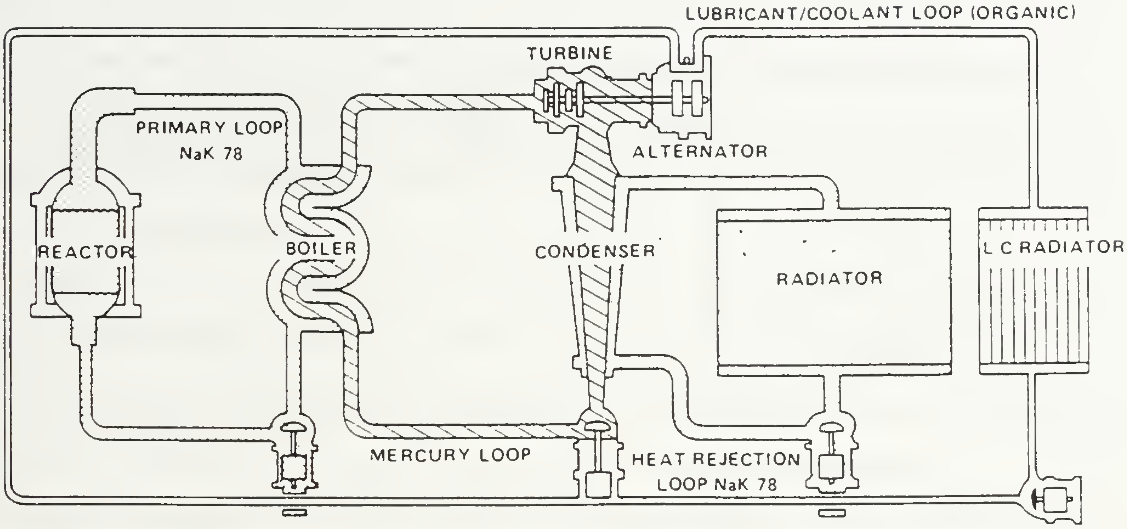
LUBRICANT/COOLANT LOOP (ORGANIC)
TURBINE
PRIMARY LOOP
NaK 78
ALTERNATOR
REACTOR
BOILER
CONDENSER
L C RADIATOR
RADIATOR
MERCURY LOOP
HEAT REJECTION
LOOP NaK 78

Figure 4-5. Fluid Loops of the SNAP-8. From (Angelo and Buden, 1985).

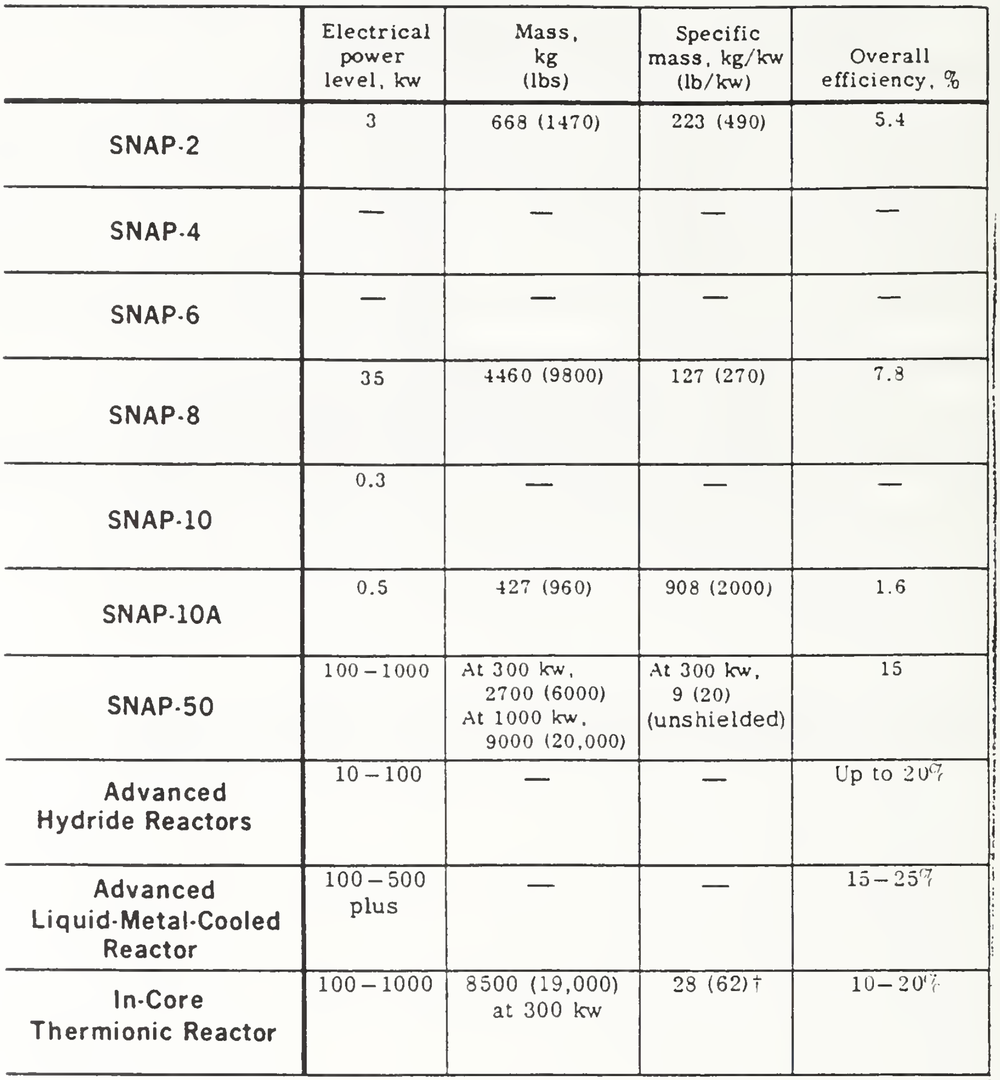

	Electrical power level, kw	Mass, kg (lbs)	Specific mass, kg/kw (lb/kw)	Overall efficiency, %
SNAP-2	3	668 (1470)	223 (490)	5.4
SNAP-4	—	—	—	—
SNAP-6	—	—	—	—
SNAP-8	35	4460 (9800)	127 (270)	7.8
SNAP-10	0.3	—	—	—
SNAP-10A	0.5	427 (960)	908 (2000)	1.6
SNAP-50	100 – 1000	At 300 kw, 2700 (6000) At 1000 kw, 9000 (20,000)	At 300 kw, 9 (20) (unshielded)	15
Advanced Hydride Reactors	10 – 100	—	—	Up to 20%
Advanced Liquid-Metal-Cooled Reactor	100 – 500 plus	—	—	15 – 25%
In-Core Thermionic Reactor	100 – 1000	8500 (19,000) at 300 kw	28 (62)†	10 – 20%

Table 4-1. Summary of SNAP Reactors. From (Corliss, 1966).

D. OTHER REACTOR DESIGNS

In addition to the uranium-dicarbide reactors of Project Rover and the uranium-zirconium-hydride reactors of SNAP, a number of other reactor designs were conceived to support space missions. They were the Rankine cycle Liquid Metal Fast Reactors, the Medium Power Reactor Experiment, the Gas-Cooled Reactor Program, the Advanced Space Nuclear Reactor Program, fluidized bed reactors, thermionic reactors, and gaseous core reactors. (Angelo and Buden, 1985)

1. Fast Reactors

Until 1973, the concept of fast neutron spectrum reactors was explored to achieve a power output capability in the range of 300 kilowatts-electric. The SNAP-50 was planned to demonstrate liquid metal cooling and achieve an electrical power rating of 10-100 kilowatts. Other reactor programs were intended to demonstrate advanced technologies for producing more power and supporting missions such as, lunar bases and electrical propulsion. This program was discontinued in 1965 and replaced by the Advanced Liquid Metal Cooled Reactor Program. All SNAP reactor programs were canceled by 1973.

The coolant used in the liquid metal-cooled reactors was lithium. Melting the lithium was found to be difficult. Temperatures of 645 K were needed prior to startup of the reactor. Uranium nitride and uranium carbide were considered as fuel materials. Both fuels encountered problems of swelling above certain temperatures and necessitated structural improvements to current fuel containment configurations. These designs used Rankine cycle converters and electromagnetic pumps in their primary and secondary loops. The secondary loop used liquid potassium as a working fluid instead of mercury. The boiler utilized a tube-in-shell heat exchanger instead of the single pass counterflow configuration. Minimizing the moisture present in the superheated, gaseous potassium as it passed through the three-stage turbine was also difficult. This series of reactor experiments validated technology for high temperature, Rankine cycle system components.

2. Advanced Space Nuclear Power Program

The Advanced Space Nuclear Power Program, called SPR, began in 1965 with the goal of exploring reactor designs that would generate up to 10 megawatts-electric. This increase in power output was intended to be accomplished by designs utilizing higher operating temperatures. The SPR-4 reactor was fueled by uranium nitride and used a Rankine cycle to convert thermal energy into 375 kilowatts-electrical. This system used sodium heat pipes to transfer heat from the reactor to the boiler. The secondary loop used potassium as a working fluid, circulated by electromagnetic pump. This reactor system was designed to be 18.8% efficient. (Angelo and Buden, 1985)

The SPR-5 reactor design used silver-tungsten heat pipes to cool the reactor core. A second set of silver-tungsten heat pipes carried thermal energy over the length of the reactor shield. At the far end of these pipes, heat was radiated to a third set of heat pipes that functioned as the emitting ends of thermionic diodes. Excess heat was them transmitted to a fourth set of heat pipes, that operated at much lower temperatures and functioned as the main radiator of the system. These extensive attempts to manage thermal energy were necessary because the reactor was designed to generate 60 megawatts-thermal in order to produce 10 megawatts-electric. Figure 4-6 provides a schematic of this heatpipe configuration.

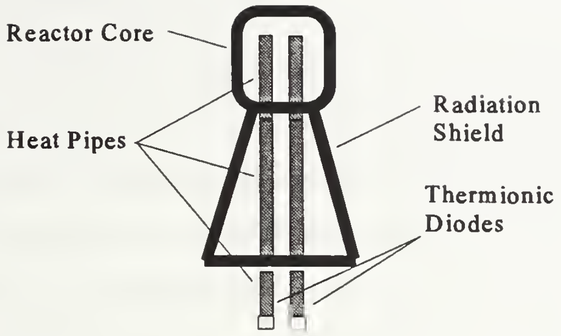

Figure 4-6. SPR-5 Reactor Heatpipes.

The SPR-6 reactor design shared the thermal rating of the SPR-5 but intended to generate only 2.5 megawatts-electrical, using a Rankine cycle converter. This design utilized a liquid lithium primary loop to cool the reactor core and transfer thermal energy to a potassium secondary loop. A heatpipe radiator was used to remove waste heat from the potassium working fluid. The SPR program was discontinued in 1968. (Angelo and Buden, 1985)

3. Thermionic Reactors

Several U.S. programs have researched the use of thermionic power conversion in nuclear reactor design. The space program of the former Soviet Union has used thermionic energy conversion extensively. Thermionic diodes are located within the perimeter of the core in an in-core design. Out-of-core designs use a heat transport system, such as heat pipes or liquid metal, to move thermal energy from the reactor core to thermionic diodes. At one phase of its development, the SP-100 program considered using thermionic conversion.

V. CURRENT NUCLEAR REACTOR PROGRAMS

A. SP-100 REACTOR PROGRAM

The termination of funding for space nuclear power programs canceled SNAP, Project Rover and other programs in 1973. In 1983, realizing that greater capabilities for generating power in space would be needed to support future missions, the Department of Energy, along with the Department of Defense and NASA, initiated the SP-100 program. The goal of this program was to develop and ground test space reactor power systems for military and civilian use. Many reactor and power conversion designs were investigated. DOE, NASA, and DOD shared the management and funding of these efforts. At the conclusion of the initial phase, in 1985, the SP-100 thermoelectric reactor power system was chosen for development. At that time, the DOD Strategic Defense Initiative Organization (SDIO) was expected to be the most likely user of the system. In the years that preceded 1992, the SP-100 program was modified due to the receipt of smaller appropriations than those expected from Congress. In the end, the program provided the United States with the option to build a space nuclear reactor capable of generating enough power to support a new class of space missions. (Young, 1992)

The SP-100 is a fast spectrum reactor, fueled by uranium nitride pellets and cooled by a lithium liquid metal coolant system designed to provide a scalable power output between 5 and 40 kilowatts. The mission life this reactor, shown in Figure 5-1, system is 7-10 years. The uranium nitride fuel pellets that power the reactor are enriched to 89% or 97% and are housed in the 978 fuel pins which make up the reactor core. The lithium liquid metal coolant flows through 42 bayonet tubes from a common header, removing heat from the core. Redundant reactor control is provided by 7 in-core safety rods and 12 radial reflectors. The liquid metal coolant, driven by an EM pump, maintains the core at 1500 K. A cross-sectional diagram of the reactor core is illustrated in Figure 5-2. (Murata, 1988)

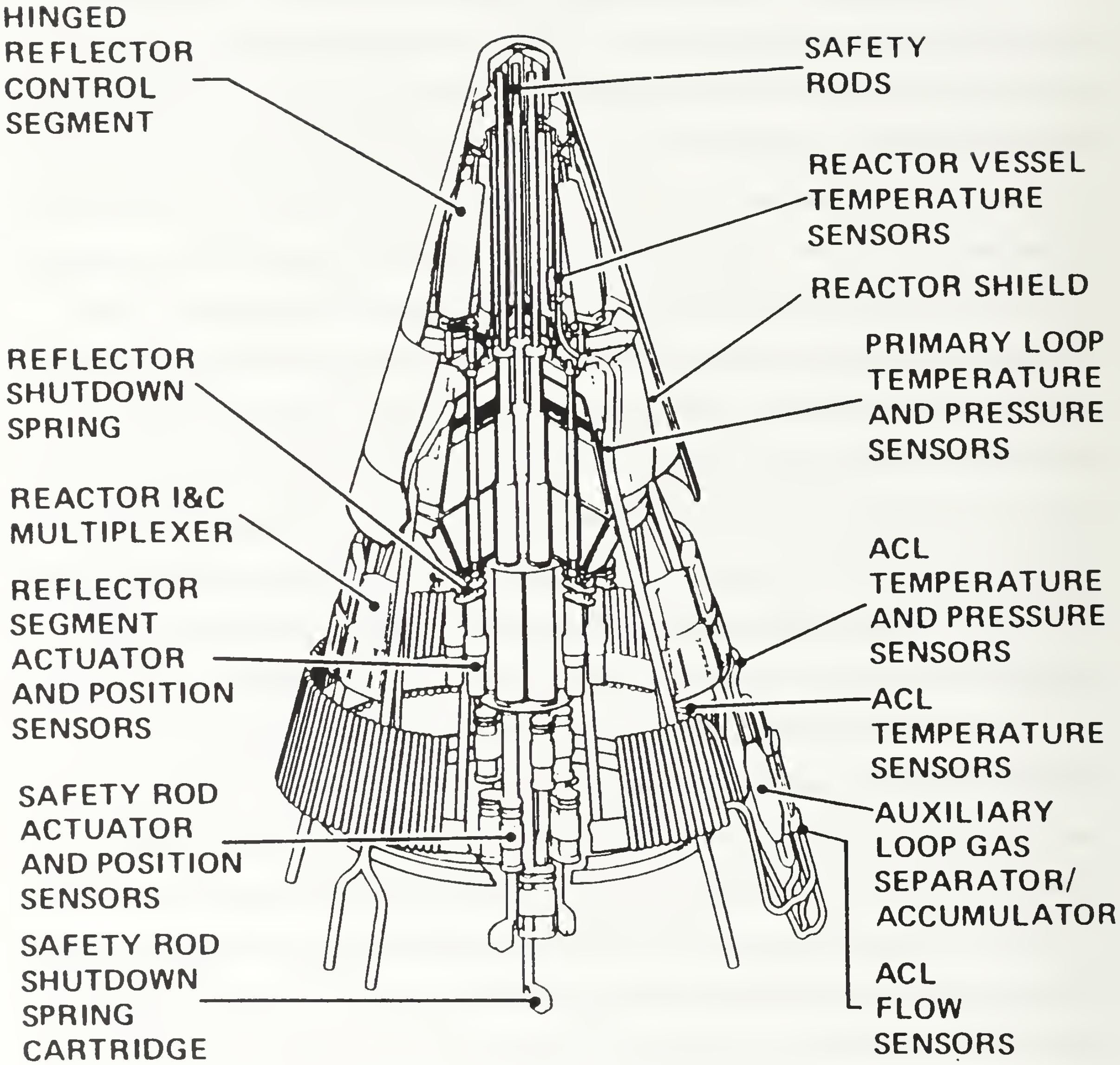
HINGED REFLECTOR CONTROL SEGMENT
SAFETY RODS
REACTOR VESSEL TEMPERATURE SENSORS
REACTOR SHIELD
PRIMARY LOOP TEMPERATURE AND PRESSURE SENSORS
REFLECTOR SHUTDOWN SPRING
REACTOR I&C MULTIPLEXER
REFLECTOR SEGMENT ACTUATOR AND POSITION SENSORS
ACL TEMPERATURE AND PRESSURE SENSORS
ACL TEMPERATURE SENSORS
SAFETY ROD ACTUATOR AND POSITION SENSORS
AUXILIARY LOOP GAS SEPARATOR/ ACCUMULATOR
SAFETY ROD SHUTDOWN SPRING CARTRIDGE
ACL FLOW SENSORS

Figure 5-1. The SP-100 Reactor. From (Armijo, 1988).

In the SP-100 system, thermal energy generated by the reactor is converted to electricity by a SiGe/GaP thermoelectric converter. Heat pipes are used to carry thermal energy from the reactor coolant to the hot junction of the thermoelectric converter. This converter subsystem is rated to an output power of 105.3 kilowatts-electrical.

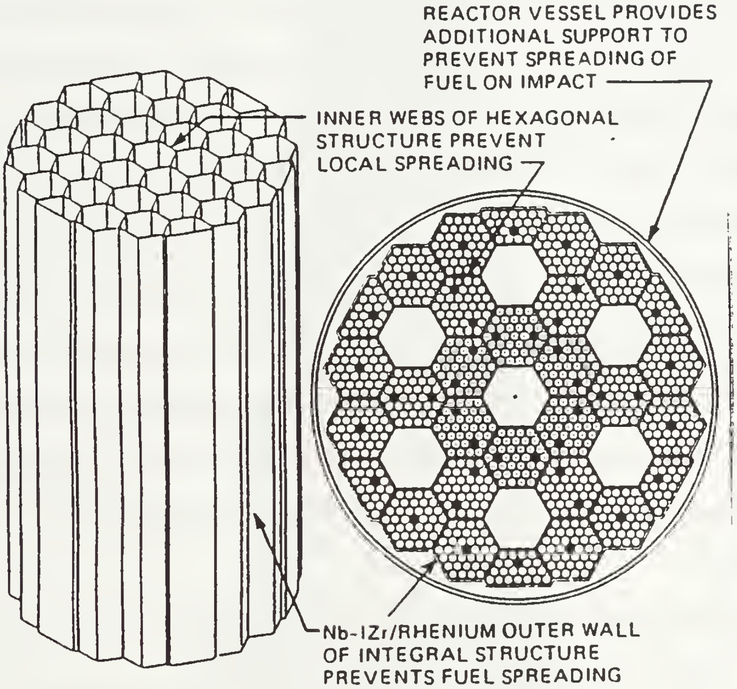
REACTOR VESSEL PROVIDES ADDITIONAL SUPPORT TO PREVENT SPREADING OF FUEL ON IMPACT
INNER WEBS OF HEXAGONAL STRUCTURE PREVENT LOCAL SPREADING
Nb-1Zr/RHENIUM OUTER WALL OF INTEGRAL STRUCTURE PREVENTS FUEL SPREADING

Figure 5-2. The SP-100 Reactor Core. From (Murata, 1988).

The liquid lithium of the secondary coolant loop carries thermal energy away from the cold junction to the radiator. The heat rejection subsystem consists of a 12-sided conical radiator with a surface area of 106.4 square meters. The reactor sits at the apex of the cone. The liquid lithium of the secondary loop flows through individual heat rejection loops in each of the 12 sides of the radiator. (Dutram, 1988)

From the beginning, the SP-100 system was designed with safety in mind. Only 4 of the 12 control reflectors are needed for reactor shutdown. The shutdown can also be accomplished by any 1 of the 7 in-core safety rods. The system is equipped with redundant electronics, drive motors, and sensors. Extensive research and modeling of potential accidents and hazards have also driven the design. The reactor core becomes radioactive only after successfully attaining orbit. (Armijo, 1988)

B. TOPAZ-II REACTOR SYSTEM

In March of 1992, Congress decided to support the purchase of a Topaz space nuclear reactor from the former Soviet Union. The purpose of the purchase would be to conduct studies of thermionic power conversion methods and to investigate the feasibility of re-modeling and certifying a Topaz reactor for flight in support of United States space nuclear power efforts. Today, the Topaz International Program located in Albuquerque, New Mexico is conducting the testing of a former Soviet Union Topaz space reactor system, designated TOPAZ-II. An illustration of the reactor is shown in Figure 5-3.

The TOPAZ-II reactor is fueled by uranium dioxide and cooled by a liquid metal sodium potassium primary loop. The reactor system provides between five and six kilowatts-electrical for a design mission life of one to three years. The uranium dioxide fuel pellets are in contained in thermionic fuel elements. The reactor core is made up of 37 individual elements each containing fuel pellets enriched to 96%. Thirty four of the elements are connected in series to drive the main electrical load. The remaining three are connected in parallel and used to power the electromagnetic pump which moves the liquid sodium potassium through the primary coolant loop. The fuel element casings incorporate a channel to allow the flow of coolant through the core. Figure 5-4 shows a cross-sectional view of the TOPAZ-II reactor core. (Venable, 1995)

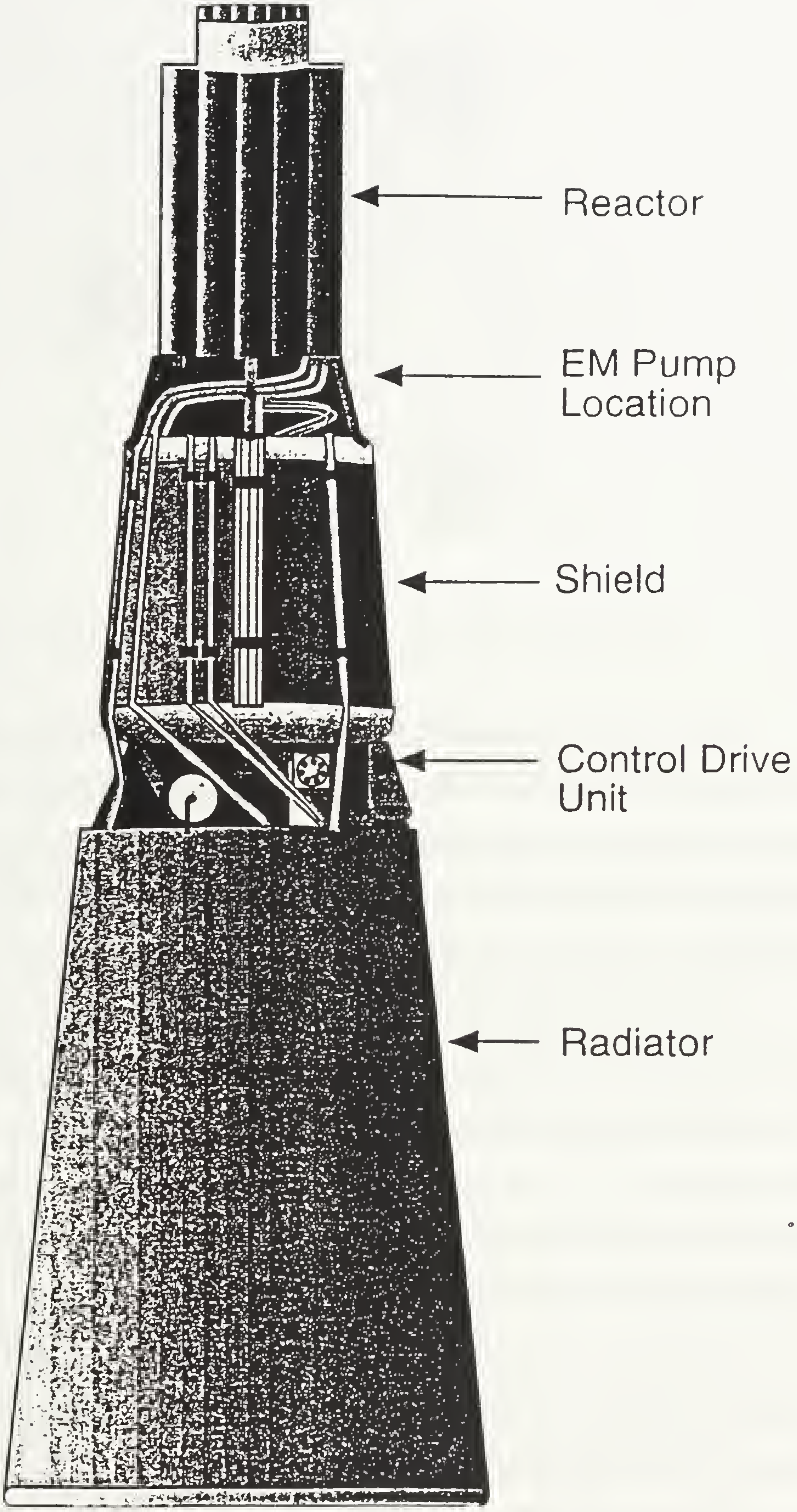
Reactor
EM Pump Location
Shield
Control Drive Unit
Radiator

Figure 5-3. The TOPAZ-II Reactor. From (Venable, 1995).

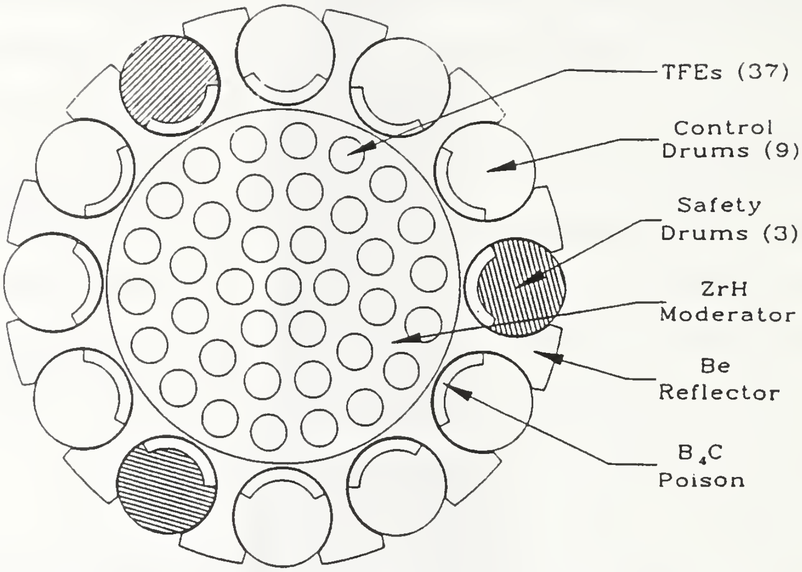

Figure 5-4. The TOPAZ-II Reactor Core. From (Venable, 1995).

The reactor is equipped with nine control drums and three safety drums. All twelve drums utilize boron carbide poison plate to control reactor operation. The safety drums are designed to face their poison plates inward until the reactor start-up commences. This ensure that the core does not enter a critical state prior to reaching orbit. The control drums regulate the reactor after initial start up. (Venable, 1995)

In this design, the energy converters are located in the reactor core. This is an example of in-core thermionics. The thermionic fuel elements, or TFE's, house both the fuel and the energy conversion apparatus. The need for a secondary loop and working fluid is eliminated. This makes the reactor system more simple. Thermionic converters operate at very high temperatures. In the TOPAZ-II core the thermionic converters operate at 1800-2100 K. The sodium potassium of the coolant loop transports the excess heat to the radiator for rejection. An earlier design of Topaz used a large single-celled thermionic converter. In the current design, each TFE is considered a single cell. The 37 individual TFE's located in the reactor core make up a multi-celled thermionic converter. Figure 5-5 illustrates the difference between single-cell and multi-cell thermionic converter configurations.

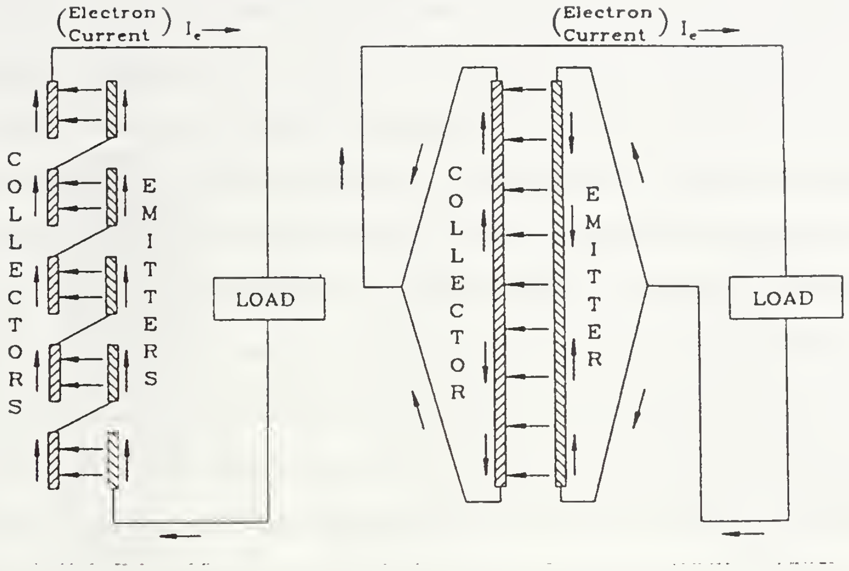

Figure 5-5. Single and Multi-cell Thermionics. From (Benke, 1994).

This configuration has demonstrated considerably higher power output and thermal efficiency than earlier, single-celled designs. The inter-electrode gap of each thermionic fuel element is filled with cesium vapor. A central cesium supply system provides the gas to each TFE from a single reservoir. This system is simple but does not allow the cesium pressure to be adjusted for an individual element. Energy density varies with location in the reactor core. Consequently, electrical power generation is not uniformly distributed among the cells. Individual TFE's can be removed and tested, but isolating parts of the array to study thermal and electrical characteristics is difficult. (Venable, 1995)

Testing of the TOPAZ-II system continues and will provide valuable information about the use of thermionic power conversion in conjunction with a space nuclear reactor.

C. SUPPORT OF CURRENT PROGRAMS

Current space nuclear reactor programs have received varying levels of support since 1983. Funding from Congress has been sporadic due to changing priorities and opinions regarding the space program. The SP-100 suffered a loss of support when Strategic Defense Initiative Organization programs ceased to be potential users. Figure 5-

6 shows a comparison between the SP-100 and TOPAZ-II nuclear reactors. Their capabilities are similar but not interchangeable. TOPAZ-II is designed to support only a one to three year mission life. This is not adequate to support certain conceptual missions, such as a manned mission to Mars. The Russians fully pursued the use of thermionic technology in the design of TOPAZ-II. The SP-100 opted for the use of thermoelectric at the conclusion of conceptual studies during the first phase of the program. It should be noted, however, that SP-100 considered the use of thermionic energy conversion and recognized that there are advantages and potential for growth in both technologies. The question of which reactor program would be of greatest benefit to the space program has not been answered. Making this decision is difficult when space missions, whose requirements would drive a reactor design, have not been committed to.

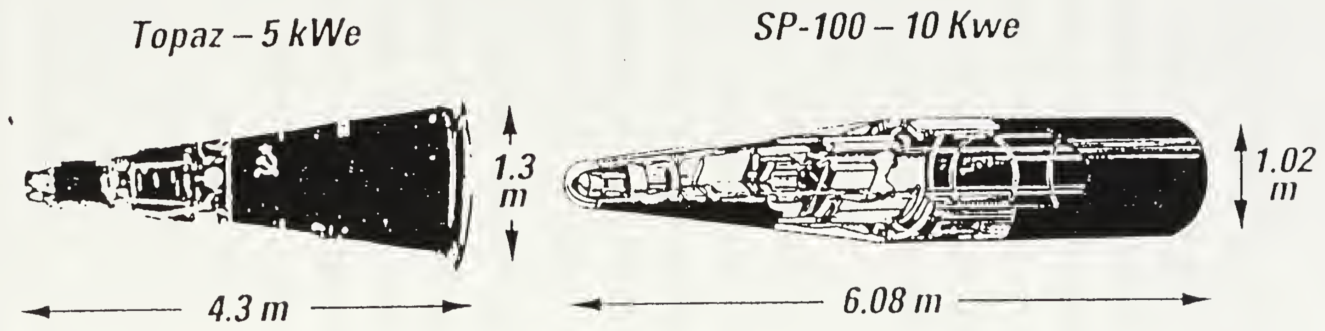

Life (yrs)	1	10 @ Full Power
Mass (kg)	1200	1060 (Comparable Equipment) 1395 w/Boom, Power Cable, Batteries, & All Power Conditioning Equip.)
Efficiency (%)	3.3 - 2.7	5 – 4.5
Radiator Area (m^2)	7.2	8.7
Safety Reqts	Soviet	U.S.
Single Point Failure Modes	EM Pump Failure	None (Multiple Self Powered Pumps)
	Radiator Leak	None (Heat Pipe Radiator Sized to Account for Meteor & Debris Puncture)
	Primary Piping Leak	None (Double Hulled Construction)
	Cesium Leak	None (Not Required)
	Hydrogen Moderator Loss	None (Not Required)

SP 084 91 471 05 (12/19)

Figure 5-6. Comparison of SP-100 and TOPAZ-II. From (Aftergood, 1988).

VI. SPACE NUCLEAR SAFETY

A. DEVELOPMENT OF EARLY SAFETY PHILOSOPHY

United States space nuclear safety policy has not evolved separately from the other applications of nuclear power. In 1956, the Joint Committee on Atomic Energy was experiencing problems with a nuclear power plant located in a Midwestern state. After reviewing that situation, the Atomic Energy Commission conducted an internal study of their safety programs. This study resulted in some legislative changes to the policies regulating nuclear power. In 1960 and 1961, the AEC reviewed the safety control and regulation of military reactors. It is an express mission of the AEC to ensure that the development of atomic energy does not create conditions that are hazardous to the safety and health of the public. This philosophy was carried forward along with other lessons learned to form what was known as Aerospace Nuclear Safety. In making the transition from regulating the safety of civilian power plants to aerospace systems, a number of special issues were considered. These issues arose from the conditions associated with the new operating environment, the developmental nature of space vehicles, the diversity of the groups in control of the space missions, and the international ramifications of all space flights. The lessons learned from the existing atomic energy program emphasized the importance of many aspects of the new safety program including, staff, standards, and public education. (Ramey, 1963)

1. Technical Staff

The AEC identified the need for an independent staff of highly trained individuals to conduct safety reviews of nuclear programs. It was made clear that the purpose of this staff was not to relieve the design teams of their responsibility to establish nuclear safety in their own programs. Safety continued to be everyone's concern. The safety staff was to add an element of skill and experience. They were specifically tasked with evaluating the most potentially dangerous aspects of a program. Review staff members served long terms in order to increase their level of knowledge and effectiveness. An emphasis was also placed upon the development of comfortable and informal relationships between safety staff members and operational team members. This was to increase to flow of information and facilitate problem solving. (Ramee, 1963)

2. Safety Standards

The establishment of standards such as, maximum radiation levels for manned missions, was a difficult task. At the time, most nuclear systems were very unique. Different operating conditions and system capabilities made it difficult to assign standards that could be applied to all systems. This situation was expected to get better with time. Experience would help to define reasonable safety standards. Weighing the potential hazards of an operation against the benefits of the operation was the basic guideline. Only low risks were considered acceptable and only when substantial gains would result from the activity. (Ramee, 1963)

3. Safety Research

Without experimental data, it would be difficult to make accurate predictions about the safety of a system. To this end, the requirement for an extensive safety testing and research program was established. This was extremely important to the development safety analysis techniques for space systems. The AEC, with the Sandia Corporation and other contractors, conducted research using methods proven by the government's weapons safety program (Ramee, 1963).

4. Public Education

One of the legislative changes that followed the Joint Committee on Atomic Energy's investigation of the problematic Midwestern powerplant required that AEC safety reports be made available to the public. Prior the Joint Committee's investigation and questions from some labor organizations, the AEC had refused to publicize safety reports. This was a difficult lesson for the AEC. Informing and educating the public became a priority. (Ramee, 1963)

B. CURRENT SAFETY POLICY

Today, space nuclear safety policy has expanded to address the use of the many different devices that have been developed since the years of the early space reactor programs. Many safety standards that were once difficult to define have been made clear through experience and research. Today, safety regulations are constructed to minimize both the probability and the impact of incidents in which radioactive materials are permitted to interact with the environment and the human population. The safety guidelines established in 1963, remain largely unchanged. However, the methods of employing this philosophy have matured considerably. Safety testing and analysis is conducted to account for all reasonably possible mishaps. (Angelo and Buden, 1985)

1. Radioisotopic Fuel Containment

When the United States first began to launch nuclear materials into space, their containers and the were designed to burn-up at the temperature of atmospheric reentry. The material would then disperse until the amount radiation exposure that would occur, should the particles be encountered, was sufficiently small. This design was superseded by the current requirement that all radioactive fuel sources remain encased and intact throughout atmospheric reentry and impact with the surface of the earth. This design ensures that the radioactive material will not come into contact with the environment. Because of this design advance, the material may be recoverable and even reusable after an accident. Advances in fuel design have also increased safety. Changing the shape of radioisotopic fuel for RTG's cermet discs and pressed material aids containment of the fuel during a potential mishap. In the event of the release of radioisotopic fuel, the U.S. safety guidelines for plutonium-238 heat sources states that the amount of fuel released shall not exceed 0.01 microcurie. One curie equals the radioactivity of one gram of pure radium. (Angelo and Buden, 1985)

2. Reactor Design and Operation

Space nuclear reactors are extremely complicated systems. Safety policy requires that all space nuclear reactors be launched in a "cold and clean" state. This means that the reactor shall be in a subcritical state until after it has achieved a safe orbit. In this subcritical state, the reactor core is not radioactive. This is a very significant safety measure as it greatly reduces the potential hazard to personnel involved with the assembly, inspection, and launch of the spacecraft. When SNAP-10A was launched in 1965, no special procedures were necessary with regards to the handling of the launch vehicle. The reactor is much like any non-nuclear payload while in the safe, inactive state. It also required that the reactor remain subcritical in the event of a launch pad explosion or if it is submerged under water. After the spacecraft reaches the desired orbit, the reactor may be started up. A reactor must be equipped with two systems that are capable of shutting the reactor down. These two systems must operate independently of each other. No environmental effect or potential explosion shall cause a space reactor core to become critical. (Angelo and Buden, 1985)

SNAP-10A, the first U.S. reactor to be launched into space, still orbits the Earth and will continue to do so for 4000 years. By the time it reenters the atmosphere, the radioactivity of its fission products will be negligible. Figure 6-1 shows the decay of these isotopes over time.

3. Safety Policy of the Former Soviet Union

In the former Soviet Union, Space Nuclear Power Systems are referred to as SNPS's. These devices are predominantly thermionic nuclear reactors. The use of nuclear power in space is known to introduce certain dangers to the public. The primary goal of their safety policy is to prevent the uncontrolled fall of a nuclear power source to earth (Angelo and Buden, 1985). In this effort to maintain nuclear powered spacecraft in safe orbits, altitude is considered to be of the greatest importance. A radiation-safe orbit is defined as one which gives a spacecraft a sufficiently long orbital life to allow the decay of fission products to reach a safe level after shutdown of the reactor. In low earth orbits, this requirement is not met. To address this, spacecrafts powered by space nuclear power systems (SNPS) in LEO are equipped with a rocket motor that will boost the satellite to a radiation-safe orbit upon completion of its mission. The secondary design precaution taken involves encasing the radioactive fuel in such a way that it will disperse and expose no more than a limited part of the population to a radiation dose not to exceed 0.5 rem per year. Doses of greater than 600 rem are lethal to most people. (Angelo and Buden, 1985)

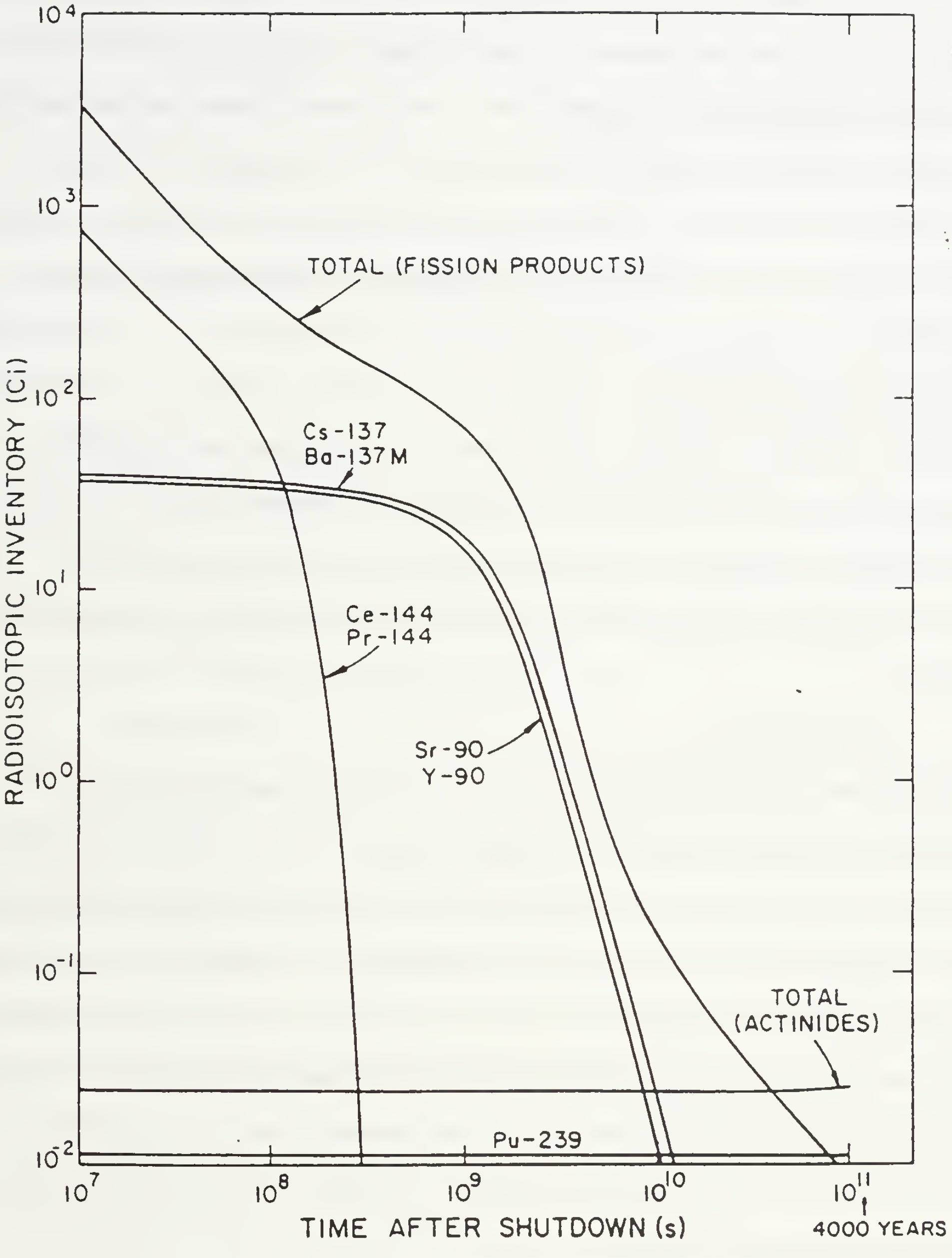

Figure 6-1. SNAP-10A Fission Products. From (Angelo and Buden, 1985).

An SNPS is designed to be safe during all modes of operation. These modes include, transportation, storage, pre-launch, launch, and normal operation. The term safe is used here to mean that in the modes prior to normal operation, the SNPS reactor will remain in a subcritical state. In the event of a pre-launch explosion, the scattering of toxic materials will be limited to the booster start area. Reactor start-up occurs only after telemetry confirms that the spacecraft is in the proper orbit. The means to shut down the reactor will be part of the design. If a reactor should fall to earth, the portion of its fission products that are not destroyed, during reentry, shall not be greater than 0.1 curies. (Gryaznov, 1989)

C. SUMMARY OF MISHAPS

The United States has launched 42 nuclear powered spacecraft since 1961. Of those missions, 41 have utilized RTG's. SNAP-10A was the first and only U.S. space reactor to fly in space (Gray,1993). Three accidents have occurred involving our spacecraft carrying RTG's. In all three situations, their safety features performed as they were designed to.

1. Transit-5BN-3

Transit-5B was the fifth RTG-powered satellite to be launched by the U.S.. In April of 1964, a malfunction of the launch vehicle's guidance control system resulted in an abort. The payload had not yet reached orbit insertion and consequently, reentered the atmosphere. The power system onboard the Transit satellite was a SNAP-9A RTG fueled by plutonium-238. The fuel entered the atmosphere in the southern hemisphere, burned up, and dispersed. The first sign of reactor material was observed four months after the abort. An aircraft being used to test the atmosphere detected plutonium dioxide at an altitude of 32.9 kilometers. The fuel had completely burned up above the West Indian Ocean. (Angelo and Buden, 1985)

2. Nimbus B-1

In May of 1968, the Nimbus B-1 meteorological spacecraft was launched from Vandenberg Air Force Base, powered by a SNAP-19 RTG. The Range Safety Officer ordered the destruction of the launch vehicle when it departed controlled flight at an altitude of 30 kilometers. The launch vehicle and its payload were tracked to impact off the coast of California. This RTG system was designed to contain its isotopic fuel in the event of reentry and impact. The generator was expected to be intact. Five months later, the SNAP-19 RTG was recovered from 90 meters of water with all of its fuel capsules undamaged. In fact, the RTG showed no signs of being adversely effected by the accident. (Angelo and Buden, 1985)

3. Apollo-13

The most recent accident involving an RTG occurred as a result of the aborted mission of Apollo-13 in April 1970. The lunar module of this spacecraft housed a SNAP-27 fueled by plutonium-238. The astronauts had used the lunar module as lifeboat following an oxygen tank explosion that caused the loss of power in the command module. When the lunar module reentered the atmosphere, the SNAP-27 fuel capsule remained intact, and came to rest in the South Pacific Ocean in a trench between six and nine kilometers deep. The environment shows no evidence of hazardous conditions as a result of its presence. (Angelo and Buden, 1985)

4. Cosmos 954

In January of 1978, a more disturbing mishap occurred. The Soviet spacecraft, Cosmos 954, reentered the atmosphere above Northern Canada and spread debris over an area of 100,000 square kilometers. The size of the reactor particles found ranged from 0.1 to 1 millimeter in diameter. Several larger fragments were found during the extensive search and were believed to come from components such as, control rods, reflectors, and cladding material. Fortunately, the debris fell mainly in Great Slave Lake and uninhabited regions. The environmental effect all of the debris found was deemed insignificant by the Canadian Atomic Energy Control Board.

This incident brought the question of the safety of space nuclear power systems to the attention of the United Nations. In 1978, the Scientific and Technical Subcommittee for the Peaceful Uses of Outer Space formed a Working Group on the Use of Nuclear Power in Space. Many aspects of the current United States space nuclear safety policy were defined in support of the working group. (Angelo and Buden, 1985)

D. INTERAGENCY SAFETY REVIEW

In April of 1965, the President issued a memorandum addressing the launch of nuclear systems into space. The purpose of this was to guarantee that President would have the opportunity to consider all aspects of any such action before it occurred. On December 14, 1977, Presidential Directive/NSC-25 established procedures for the conduct of technological experiments with the potential to cause adverse environmental effects. This included the launch of nuclear systems into space (Brzezinski, 1977). This document described the process to be used by agencies to report to Office of Science and Technology Policy and it identified activities that require the approval of the President. The directive also called for the formation of a safety review panel with members from the Department of Defense, the Department of Energy, and NASA. The purpose of the Interagency Nuclear Safety Review Panel (INSRP) would be to evaluate the risks associated with the activities regulated by the directive.

Today, any agency sponsoring the launch of a spacecraft containing radioactive sources above thresholds set by the directive must obtain permission from the President, through the Office of Science and Technology Policy. The agency must also conduct a safety review and complete a Final Safety Analysis Report (FSAR). The INSRP reviews this report and independently evaluates the safety risk of the program. The INSRP's findings are recorded in a separate Safety Evaluation Report (SER) and submitted with the FSAR to the President for launch approval (Frank et al., 1996). Calculating risk is the function of these procedures.

Risk is defined, by INSRP, as the uncertainty of the frequency at which undesired events may occur. The primary undesired event, that concerns INSRP, is an incident which causes the population to suffer radiological health effects, specifically, cancer fatalities. The secondary concern is the contamination of land by toxic material and the cost of decontamination. The INSRP is divided into five subpanels based upon the aspects of risk assessment they are responsible for. Each subpanel performs a step in the process of generating the SER. Figure 6-2 illustrates the organization of INSRP and the assignment of risk assessment tasks to each of the subpanels. As the figure shows, risk assessment is thought of in six elements. The entire process involves extensive modeling and probability techniques, as well as conventional engineering experimental methods. (Frank et al., 1996)

1. Accident and Environment Definition

Scenarios modeling launch, reentry, and fly-by accidents are generated and the frequency and uncertainty of their occurrence is calculated. Any accident scenario that could damage the nuclear system is considered. Uncertainty in these scenarios is introduced by modeling assumptions and performance ratings of equipment. The techniques used in this process include, statistical methods, failure mode and effects analysis, and Monte Carlo methods. The loads due to shock, impact, thermal gradients, and overpressure must be estimated in order to characterize the environments that would result from an accident. (Frank et al., 1996)

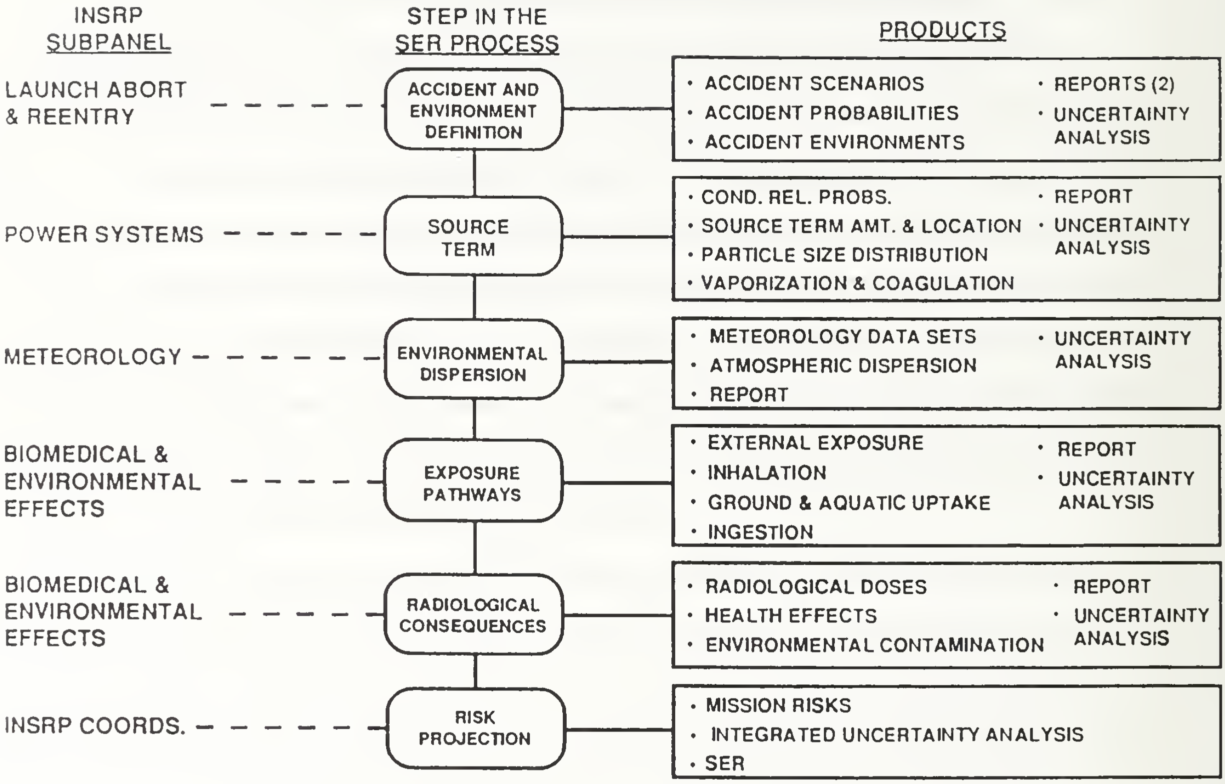
INSRP SUBPANEL
STEP IN THE SER PROCESS
PRODUCTS
LAUNCH ABORT & REENTRY
ACCIDENT AND ENVIRONMENT DEFINITION
• ACCIDENT SCENARIOS
• ACCIDENT PROBABILITIES
• ACCIDENT ENVIRONMENTS
• REPORTS (2)
• UNCERTAINTY ANALYSIS
POWER SYSTEMS
SOURCE TERM
• COND. REL. PROBS.
• SOURCE TERM AMT. & LOCATION
• PARTICLE SIZE DISTRIBUTION
• VAPORIZATION & COAGULATION
• REPORT
• UNCERTAINTY ANALYSIS
METEOROLOGY
ENVIRONMENTAL DISPERSION
• METEOROLOGY DATA SETS
• ATMOSPHERIC DISPERSION
• REPORT
• UNCERTAINTY ANALYSIS
BIOMEDICAL & ENVIRONMENTAL EFFECTS
EXPOSURE PATHWAYS
• EXTERNAL EXPOSURE
• INHALATION
• GROUND & AQUATIC UPTAKE
• INGESTION
• REPORT
• UNCERTAINTY ANALYSIS
BIOMEDICAL & ENVIRONMENTAL EFFECTS
RADIOLOGICAL CONSEQUENCES
• RADIOLOGICAL DOSES
• HEALTH EFFECTS
• ENVIRONMENTAL CONTAMINATION
• REPORT
• UNCERTAINTY ANALYSIS
INSRP COORDS.
RISK PROJECTION
• MISSION RISKS
• INTEGRATED UNCERTAINTY ANALYSIS
• SER

Figure 6-2. Organization of INSRP. From (Frank et al., 1996).

2. Source Term

Using the loads determined to be present in each of the accident scenarios, INSRP assesses the potential damage to the nuclear system. The goal of this process is to determine if nuclear material would be released. Important factors in the characterization of the source term are the type of fuel used by the system, its chemical composition, the amount released, its particle size, dispersion patterns, and the probability of release. (Frank et al., 1996)

3. Environmental Dispersion

The degree to which released fuel would disperse is calculated through the analysis of meteorological and atmospheric conditions. These conditions cannot be determined in advance, so their effect upon the potential dispersal of released fuel is probabilistic. The goal of this analysis is to calculate the predicted dose of radiation that be received by the population for a given accident scenario (Frank et al., 1996).

4. Exposure Pathways

The dose of radiation predicted by the environmental dispersion analysis serves as the input for the analysis of exposure pathways. This is an evaluation of the effect that released radioactive material would have on the population and on the environment. Human uptake is the exposure of humans to the material through ingestion. It's magnitude is measured by the number of latent cancers that would result. Estimations assume that areas are not evacuated and that ground decontamination efforts are not made.

5. Radiological Consequences

The impact of the release of radioactive material upon the population is measured by the number of human health effects. These effects are incidences of latent cancer in individuals which may be fatal. This number cannot ever be zero, because there is never zero risk. Variability and uncertainty are introduced into this analysis by inherent differences in human susceptibility to radiation and uncertainties related to the models and assumptions employed.

6. Risk Projection

The procedures of the previous five sections are components of the overall risk evaluation of a launch mission. A flow chart, in Figure 6-3, illustrates the process. The end result of the analysis is a set of probability curves, shown in Figure 6-4. The multiple accident scenarios. Certain elements that effect the outcome of a mishap, such as meteorological conditions, vary greatly and cannot be predicted with accuracy. The 95% confidence curve represents the results of events occurring in the worst possible conditions. This is the most conservative risk assessment. The 5% confidence curve represents the results of events occurring under the most favorable of circumstances. This is the most optimistic risk assessment. (Lyver, 1996)

To understand the representation of Figure 6-4, suppose that this mission was repeated over and over again. Theory predicts, with 95% confidence, that a mishap resulting in the death of one person will occur approximately once every 100,000 missions. This is denoted by point 1 in the figure. Theory predicts, with 5% confidence, that an accident of this seriousness will occur only once in 5,000,000 missions. This is the interpretation of point 2 in the figure.

The risk analysis data is then incorporated into the final report. The Safety Evaluation Report (SER) is the summary of the INSRP's risk assessment of the mission. Then, INSRP, also comments on the accuracy of safety review conducted by the sponsoring agency.

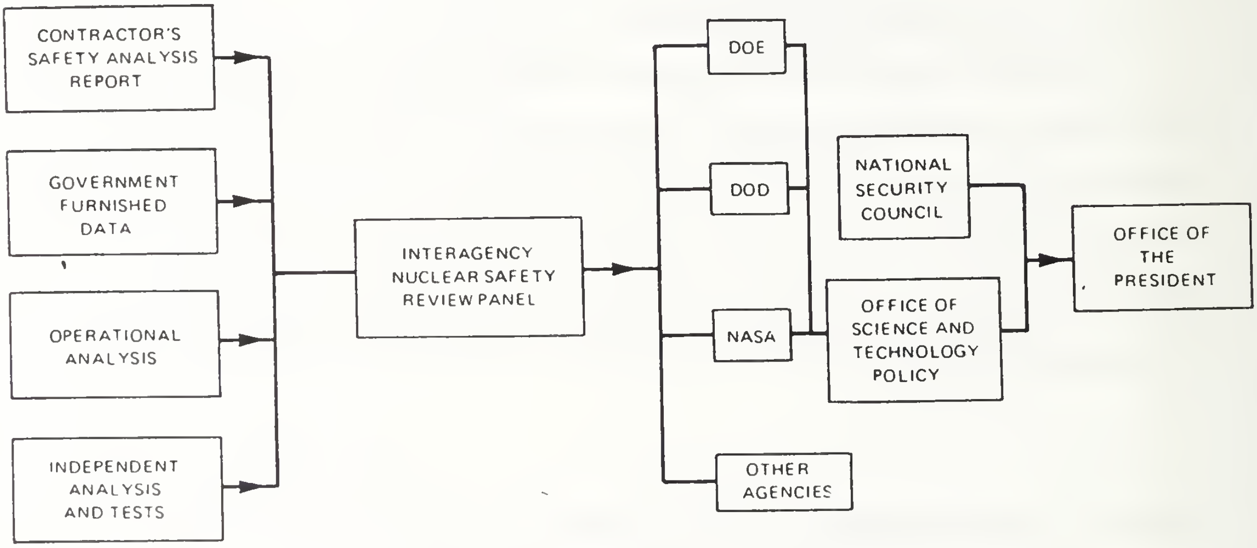
CONTRACTOR'S SAFETY ANALYSIS REPORT
GOVERNMENT FURNISHED DATA
OPERATIONAL ANALYSIS
INDEPENDENT ANALYSIS AND TESTS
INTERAGENCY NUCLEAR SAFETY REVIEW PANEL
DOE
DOD
NASA
OTHER AGENCIES
NATIONAL SECURITY COUNCIL
OFFICE OF SCIENCE AND TECHNOLOGY POLICY
OFFICE OF THE PRESIDENT

Figure 6-3. The Safety Review Process. From (Frank et al., 1996).

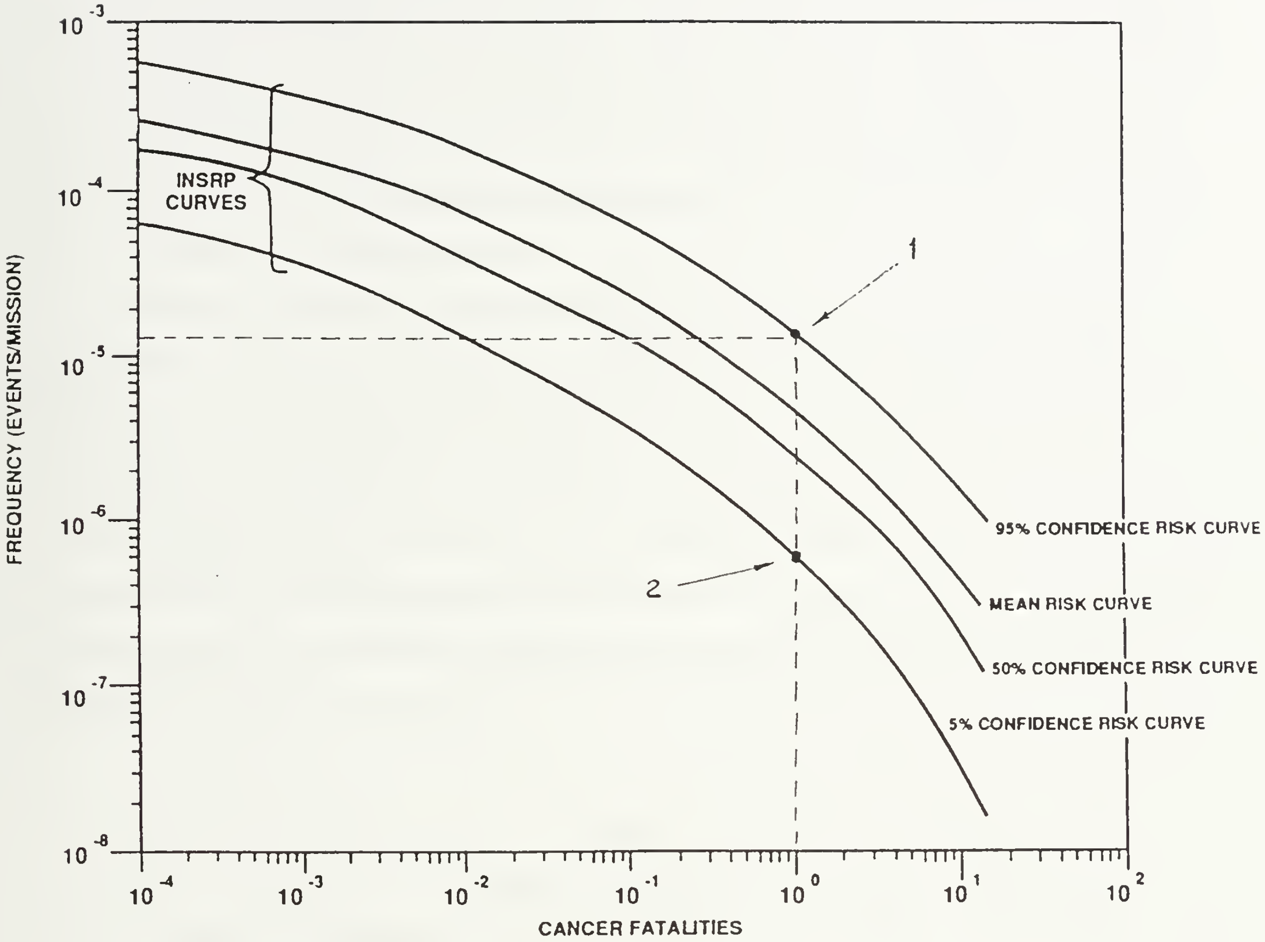

Figure 6-4. Risk Assessment Results. From (Frank et al., 1996).

VII. CONCLUSIONS

Programs for the development and construction of space nuclear power systems have received sporadic funding and support in the United States. This lack of enthusiasm seems to stem from doubts that can be grouped into two categories. The first is made up of questions about the safety and controllability of nuclear systems. The second group of questions is concerned with the utility and necessity of these power systems.

A. SAFETY AND REGULATION

The safety of space nuclear systems is best proven by historical data. Table 7-1 summarizes the use of space nuclear power systems by the United States and the former Soviet Union. The Russians have used space reactors in low-earth orbit extensively. There are 26 reactors in orbit now. When they have completed their missions, they are boosted to higher orbits where they stay. It is important to understand that once these reactors are in a safe orbit, they will not come down for thousands of years, by which time the fuel products have decayed to a harmless level of radiation. The U.S. space reactor SNAP-10A is in such an orbit now.

	USSR[1]		USA	
	RTGs	REACTORS	RTGs	REACTORS
PRESENTLY IN ORBIT	2	26	11	1
FAILED TO LAUNCH	2	2	2	0
REENTERED	0	2	2	0
ON MOON	2	0	5	0
ON MARS	0	0	4	0
INTERPLANETARY	0	0	17	0
TOTAL LAUNCHED	6	30	41	1

Table 7-1. Current Use of Space Nuclear Power. From (Gray, 1993).

The previous chapter discussed four mishaps involving nuclear power sources in detail. In every one of these situations, the system performed as it was designed to. Safety measures can ensure burn-up and dispersal or containment of the nuclear fuel. We can design systems to behave either way. We have decided that it is better to contain the fuel throughout reentry and impact and this design has proven to be effective, twice.

It is also important to know that the use of nuclear sources for space applications is regulated with extreme strictness. The degree of strictness could even be of a nature to discourage their use. All nuclear sources of a certain potency must be reported to the White House via the Office of Science and Technology before they can be launched aboard a spacecraft. To understand where this threshold is set, consider a common, home smoke detecting device. These devices contain a very small amount of the radioisotope, Am-241. The level of radioactivity, 0.5 microcuries, is so small that they are available in retail stores without warning labels or special instructions. The space shuttle employs 19 of these same devices. The personnel at NASA must submit a formal report to OST before each launch (Lyver, 1996). There seems to be a general lack of understanding about safety as it applies to nuclear energy. Space nuclear safety policy has been in place for years, educating the public is necessary to gain political support for this source of power.

B. UTILITY OF SPACE NUCLEAR POWER

The trend in exploration spacecraft design has tended towards micro-technology. Advances in solar cell and battery efficiencies have made more power available. Advanced power budgeting and thermal control further optimize the use of power. However, these efforts are not bringing space power systems to a new quantum level. At distances far from the Sun, it is not feasible build a solar array large enough support a manned mission deep into space. As Figure 7-1 illustrates, conventional sources simply cannot generate as much power as nuclear systems can.

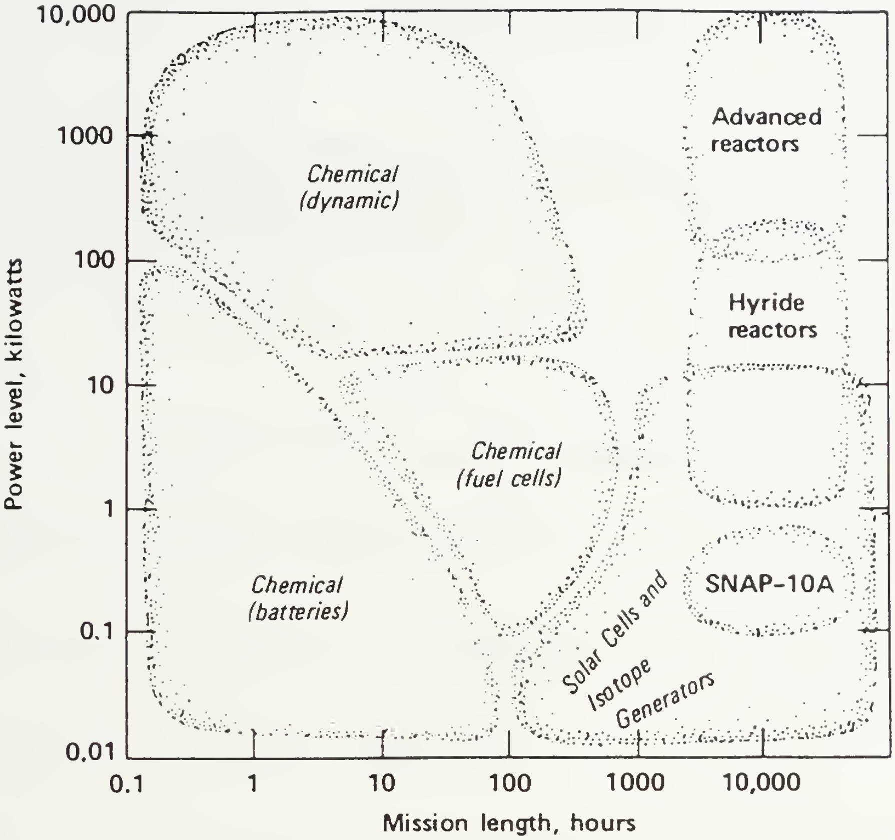

Figure 7-1. Methods of Space Power Generation. From (Corliss, 1966).

C. RECOMMENDATIONS

Lack of understanding is a great obstacle to the use of nuclear energy in space. Space nuclear safety policy has been in place for years, educating the public is necessary to gain political support for this source of power.

If we intend to explore space further with manned and unmanned spacecraft, the development of space nuclear power must continue steadily. One of the benefits of these efforts will be the development of safe, powerful, systems that will have great use in earth-orbiting applications.

The arguments against the use of space nuclear power systems are more political in nature than technical. Public unpopularity due to perceived safety risks and high monetary costs, result in a reluctance to push forward to a new level space exploration.

LIST OF REFERENCES

Aftergood, Steven (1992) "Testimony of the Senior Research Analyst, Federation of American Scientists on the Future for the SP-100 Space Reactor Program," Presented at the *Hearing Before the Subcommittee on Investigations on Science, Space, and Technology, U.S. House of Representatives*, March 12, 1992.

Angelo, J. A. and D. Buden (1985) *Space Nuclear Power*, Orbit Book Company, Malabar, FL.

Angrist, S. W. (1965) *Direct Energy Conversion*, Allyn and Bacon, Inc., Boston, MA.

Armijo, S. (1988) "Project Highlights," Presented at the *SP-100 Project Integration Meeting*, 19-21 July, 1988, Long Beach, CA.

Benke, S. M. (1994) "Operational Testing and Thermal Modeling of a TOPAZ-II Single-Cell Thermionic Fuel Element Test Stand," Naval Postgraduate School, Monterey, CA.

Brzezinski, Z. (1977) Presidential Directive/NSC-25

Corliss, W. R. (1966) *Nuclear Reactors for Space Power*, United States Atomic Energy Commission, Division of Technical Information, Washington, D.C.

Culp, A. W., Jr. (1979) *Principles of Energy Conversion*, McGraw-Hill Book Company, San Francisco, CA.

Frank, M. V. et al. (1996) "An Overview of the Space Nuclear Risk Assessment and Review Process of the Interagency Nuclear Safety Review Panel, Office of the NASA INSRP Coordinator, Washington, D.C.

Gray, L. B. (1993) "Possible Accident Consequences," Presented at the *Interagency Working Group for Space Nuclear Power*, 15 December, 1993.

Gryaznov, G. M. (1989) "The Nuclear and Radiation Safety Concept for Thermionic Space Nuclear Power Systems," in *Proc. 6th Symposium of Space Nuclear Power Systems*, M. S. El-Genk and M. D. Hoover, eds., Albuquerque, NM.

Lyver, J. W., IV (1996) Personal Communication, NASA Headquarters, Washington, D.C.

Michael, S. (1996) Personal Communication, Naval Postgraduate School, Monterey, CA.

Murata, R. (1988) "Reactor Subsystem," Presented at the *SP-100 Project Integration Meeting*, 19-21 July, 1988, Long Beach, CA.

Pedersen, E. S. (1964) *Nuclear Energy in Space*, Prentice-Hall, Inc., Englewood Cliffs, NJ.

Ramey, J. T. (1963) "Aerospace Nuclear Safety- Lessons from Civilian and Military Reactor Experience," in *Proc. Aerospace Nuclear Safety, National Topical Meeting*, R. E. Dunlap, ed., American Nuclear Society, Albuquerque, NM.

Samson, (1997) Personal Communication, Monterey, CA.

Venable, J. R. (1995) "Electrical Characteristics and Thermal Analysis of a TOPAZ-II Single-Cell Thermionic Fuel Element Test Stand," Naval Postgraduate School, Monterey, CA.

Young, W. H. (1992) "Testimony of the Assistant Secretary for Nuclear Energy, U.S. Department of Energy on Space Reactor Power Systems Program," Presented at the *Hearing before the Subcommittee on Investigations on Science, Space, and Technology, U.S. House of Representatives*, March 12, 1992.

Zemansky, M. W. (1957) *Heat and Thermodynamics*, McGraw-Hill, San Francisco, CA.

INITIAL DISTRIBUTION LIST

		No. Copies
1.	Defense Technical Information Center 8725 John J. Kingman Rd., STE 0944 Ft. Belvoir, VA 22060-6218	2
2.	Dudley Knox Library Naval Postgraduate School 411 Dyer Rd. Monterey, CA 93943-5101	2
3.	Chairman Department of Aeronautical and Astronautical Engineering Naval Postgraduate School Monterey, California 93943-5106	1
4.	Professor Oscar Biblarz Department of Aeronautical and Astronautical Engineering, Code AA/Bi Naval Postgraduate School Monterey, California 93943-5106	1
5.	Professor Sherif Michael Department of Electrical and Computer Engineering, Code EC/Mi Naval Postgraduate School Monterey, California 93943-5000	2
6.	Professor Barry Leonard Department of Aeronautical and Astronautical Engineering, Code AA/Lb Naval Postgraduate School Monterey, California 93943-5000	2
7.	Frederick Gregory NASA Headquarters, Code Q Washington, D.C., 20056	1
8.	LT Joseph P. Reason, Jr. 1651 Dillingham Blvd. Norfolk, Virginia 23511-3004	2

9. LT Brigitte Horner 1
612 Thunderbird Ct., Apt. A
Chesterfield, Missouri 63017

DUDLEY KNOX LIBRARY
NAVAL POSTGRADUATE SCHOOL
MONTEREY CA 93943-5101

DUDLEY KNOX LIBRARY
3 2768 00339472 7